INTERNATIONAL JOURNAL OF CONTROL
2022, VOL. 95, NO. 7, 1898–1912
https://doi.org/10.1080/00207179.2021.1885741

Taylor & Francis
Taylor & Francis Group

Robust adaptive input-output control for a class of modular robotic systems via inverse optimality theory

Jiamin Wang, Yujiong Liu and Pinhas Ben-Tzvi

Robotics & Mechatronics Lab, Department of Mechanical Engineering, Virginia Tech, Blacksburg, VA, USA

ABSTRACT

This paper introduces a model-based robust adaptive input-output control framework for a family of robotic systems that include under-actuation, nonholonomic, and constrained properties. The proposed control framework can provide fast and effective controller generation for modular robotic systems (MRS) with interchangeable subsystems. The controller was first derived based on the general properties of nonholonomic robotic dynamic models while considering under-actuation and constraints. Then the adaptive control technique is introduced to overcome the effects such as inertia and force uncertainties. Robust augmentation is implemented via inverse optimality theory, which is verified with respect to a meaningful cost function. A simulation study on an aerial manipulator system with model uncertainty and disturbance was provided to demonstrate the characteristics and effectiveness of the proposed controller.

ARTICLE HISTORY
Received 20 December 2018
Accepted 30 January 2021

KEYWORDS
Model-based control; adaptive control; robust control; inverse optimality; modular robotic system

1. Introduction

Modular and reconfigurable robotic systems (Davey et al., 2012; Moubarak & Ben-Tzvi, 2012; Wei et al., 2011; Yim et al., 2007) free robots from being constrained to a fixed structure design, and thereby allow assembling different robotic modules into different configurations for different applications. A typical example of this concept is presented in Figure 1, where an aerial manipulator is assembled from UAV and manipulator subsystems. Note that this setting is very similar to the classic spacecraft-manipulator problem (H. Wang, 2011) except that for modular robotic systems (MRS), the modular components could have various types and quantities, and they could be coupled with various constraints. This unique characteristic of MRS leads to the modelling and control challenges that they need to consider various modules and constraints as well as their combinations.

An efficient way to address the modelling challenge is to model each module separately and then, depending on the configuration, combine the individual dynamics using constraints (Shah et al., 2012). This way, the vast model space problem is simplified to a combinatorial problem of finite dynamic model libraries. More importantly, the individual dynamics usually can be modelled beforehand, making this approach more flexible than the whole-body modelling approach (Buschmann et al., 2006). However, introducing constraints into the system will inevitably result in redundancy of states and sometimes involve nonholonomic constraints and under-actuation (e.g. the quad-arm modules in Figure 1). Therefore, an essential feature to address the control challenge is to provide a solution for a *constrained*, *nonholonomic* and *under-actuated* robotic system.

Control methods that require configuration specific training (Melek & Goldenberg, 2003; Peters et al., 2003) and planning (Guo & Woo, 2003; Sugeno, 1985) are not usually applicable for this problem, which leads to the selection of model-based control (MBC). However, MBC may not perform well in practice due to model uncertainties and disturbances. Therefore, adaptiveness and robustness are introduced to improve the practicability of controllers. A variety of adaptive control methods have been widely studied and explored over years, as they are frequently applied in control systems for various complex systems such as spacecrafts (Slotine & Di Benedetto, 1990; Yoon & Tsiotras, 2008) and robots (Ortega & Spong, 1989; Slotine & Li, 1987). While a few researchers considered the constraint characteristic (Arimoto et al., 1993; Whitcomb et al., 1997) and under-actuation characteristic (Gu & Xu, 1995; K. D. Nguyen & Dankowicz, 2015) cases separately, the adaptive control for systems with both characteristics is a relatively less explored topic.

Amongst the existing robust control methods, nonlinear robust control deals with the nonlinearity of the system directly. As a class of nonlinear optimal control problems (Aliyu, 2011; Freeman & Kokotovic, 2008; Lewis et al., 2012), some nonlinear robust controllers require solving the Hamilton-Jacobi-Isaac (HJI) partial differential equation introduced by their cost functions, which remain a challenge since the current algorithms (such as State Dependent Riccati Equation (SDRE) (Cloutier, 1997; Xin & Balakrishnan, 2005)) cannot guarantee a globally optimal solution. Alternatively, inverse optimality approaches the solution with respect to a meaningful performance function based on a stabilising Control Lyapunov Function (CLF), which does not require online calculation and can obtain a globally optimal solution. The technique has been applied to multibody systems such as spacecrafts (Luo et al., 2005) and legged robots (Ames et al., 2014; Q. Nguyen

CONTACT Pinhas Ben-Tzvi bentzvi@vt.edu Robotics & Mechatronics Lab, Department of Mechanical Engineering, Virginia Tech, Blacksburg, VA 24060, USA

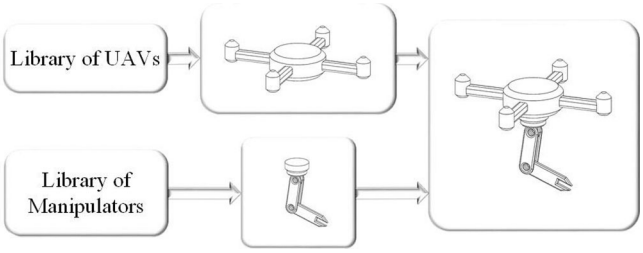

Figure 1. A modular robotic system (aerial manipulator) combined from compatible modules.

& Sreenath, 2015). This also provides a potential solution for the robust adaptive control framework, which has not yet been fully explored.

Therefore, this paper focuses on applying the existing inverse optimal robust adaptive control technique on a class of MRS, for which the whole body dynamics usually incorporates nonholonomic constraints and under-actuation. Focusing on this unique problem with considerations such as model uncertainties and external disturbances usually apparent in MRS, this paper solves the problem by designing an inverse optimal robust adaptive controller. More specifically, the proposed controller has the following features:

(F1) The control law is applicable to a wide range of robotic systems due to the more general nonholonomic constraints and under-actuation characteristics.
(F2) A systematic adaptive control approach is established for overcoming model uncertainties in the system's inertia properties and generalised forces, and guarantees error convergence and adaptive parameters under proper conditions.
(F3) $\mathcal{H}_\infty$ robustness augmentation is applied for $\mathcal{L}_2$ disturbance attenuation via inverse optimal theory. The integrated controller is proven to be globally optimal for a meaningful cost function that leads to a global asymptotic convergence of the corresponding robust adaptive control Lyapunov function (RACLF).

A sample simulation case on the aerial manipulator system shown in Figure 1 was studied to validate the proposed controller framework.

The outline of the remainder of this paper is as follows. Section 2 first reviews the necessary theoretical background of MRS dynamics, model-based control, and the inverse optimality for robust adaptive control, and then formulates the core problem to be solved. Section 3 discusses the robust adaptive controller design and the proof of inverse optimality. Section 4 provides the simulation case-study of an aerial manipulator, and Section 5 draws the conclusion of this research.

2. Theoretical background and problem statement

This section presents the necessary theoretical background for model-based control and robust adaptive controller through inverse optimality. These two components constitute the foundation of the proposed controller in Section 3. The notations used in this paper are shown in Table 1.

Table 1. Mathematical notations.

$\|z\|$	Euclidean norm of vector z
$z_1 \times z_2$	Multiplications of quaternions z_1 (4×1) and z_2 (4×1)
$\bar{z}$	Conjugation of quaternion z (4×1)
$z_{m\times n}$	A $m \times n$ matrix with all elements as $z \in \mathbb{R}$
I_n	Identity matrix of rank n (dimensions fit in its block if no subscript)
Z^{-T}	Inverse of the transpose of square matrix Z
Z^+	Moore-Penrose pseudo inverse of a matrix Z
$Z > 0$	Square matrix Z is positive definite
$Z < 0$	Square matrix Z is negative definite
$\|Z\|$	$\mathcal{L}_2$ norm of matrix Z
$L_Y Z$	Lie derivative of function $Z(x)$ with respect to function $Y(x)$
$\{X \backslash Y\}$	The set of X excluding set Y where $Y \subset X$

2.1 Modular robotic system dynamics and model-based control

The dynamical model of a robotic system can be written as (Griffin & Grizzle, 2017; Kane & Levinson, 1985; Kurdila & Ben-Tzvi, 2019)

$$M(q,\xi)\ddot{q} = H(q,\dot{q},\xi) + J_u^T(q,\xi)u + J_\lambda^T(q,\xi)\lambda \tag{1a}$$

$$\dot{\xi} = J_\xi(q,\xi)\dot{q} + \Omega_\xi(q,\xi) \tag{1b}$$

where $q \in \mathbb{R}^{n_q}$ is the generalised coordinate vector; $u \in \mathbb{R}^{n_u}$ is the control input; $M \in \mathbb{R}^{n_q \times n_q}$ is the inertia matrix, which is positive definite; $H \in \mathbb{R}^{n_q}$ is the unified generalised force, which involves Coriolis forces, centripetal forces, potential energy forces, and energy dissipation forces, etc.; and $J_u \in \mathbb{R}^{n_u \times n_q}$ is the input Jacobian matrix. Note that Equation (1) follows a nonholonomic formulation by adopting Equation (1b) that governs the dynamics of the nonholonomic state $\xi \in \mathbb{R}^{n_\xi}$, where $J_\xi \in \mathbb{R}^{n_\xi \times n_q}$ is the nonholonomic Jacobian, and $\Omega_\xi \in \mathbb{R}^{n_\xi}$ is the remaining nonlinear term of q and ξ. An example of the nonholonomic state is the quaternion, which is often used to describe the 3D rotation (Fresk & Nikolakopoulos, 2013). The relationship between the quaternion coordinate $\xi_{\text{quat}} \in \mathbb{R}^4$ and the angular velocity $\omega_{\text{quat}} \in \mathbb{R}^3$ can be written as

$$\dot{\xi}_{\text{quat}} = 0.5(\xi_{\text{quat}} \times \begin{bmatrix} 0 & \omega_{\text{quat}}^T \end{bmatrix}^T) \tag{2}$$

Therefore, the quaternion cannot be explicitly expressed in terms of the integral of angular velocity.

For systems with multiple modules, an easy way to acquire the whole body dynamics is to assemble the modular component dynamics directly with appropriate constraints. For a system with n modules, the dynamical model from Equation (1) can be constructed with the dynamical terms of its subsystems through

$$\text{for } X = M, J_u, J_\xi : X = \text{diag}(X_1, X_2, \ldots, X_n)$$

$$\text{for } X = q, \xi, u, H, \Omega_\xi : X = [X_1^T, X_2^T, \ldots, X_n^T]^T$$

where X_i ($i = 1, 2, \ldots, n$) stands for a dynamical term (vector or matrix) from the model equation Equation (1) of ith module; $X = \text{diag}(X_1, X_2, \ldots, X_n)$ denotes having square matrices X_i as the diagonal components of the block matrix X, which is a dynamical term of the assembled system. Therefore, the assembled dynamical model incorporates all the model information of its modules. Modelling modular robot dynamics using this

approach has the advantage of being able to quickly acquiring the dynamics of the whole system without remodelling or rearranging individual properties. For instance, the inertial matrix inverse can be obtained efficiently by processing the individual inertial matrix of each module in parallel, and applying the diagonal block matrix

$$M^{-1} = \mathrm{diag}(M_1^{-1}, M_2^{-1}, \ldots, M_{n-1}^{-1}, M_n^{-1}) \tag{3}$$

The coupling and interaction between the module dynamics are realised with the Lagrange multiplier (constraint force) $\lambda \in \mathbb{R}^{n_\lambda}$. The constraint force and its direction characterised by $J_\lambda \in \mathbb{R}^{n_\lambda \times n_q}$ are obtained from the constraint equations. The dynamic model in Equation (1) is compatible with nonholonomic constraints, as long as these constraints follow the representation in terms of the time derivatives as shown in Equation (4), where $r_\lambda : \mathbb{R}_+ \times \mathbb{R}^{n_q} \times \mathbb{R}^{n_q} \times \mathbb{R}^{n_\xi} \to \mathbb{R}^{n_\lambda}$ is the constraint reference vector.

$$\dot{r}_\lambda(t, q, \dot{q}, \xi) = J_\lambda(q, \xi)\dot{q}; \quad \ddot{r}_\lambda = J_\lambda \ddot{q} + \dot{J}_\lambda \dot{q} \tag{4}$$

In most cases, $\ddot{r}_\lambda = 0$; however, it may not necessarily be zero if the constraint is defined as time varying or state dependent. Based on these properties, the constraint force can be derived by substituting the $\ddot{q}$ from Equation (1a) into Equation (4), which results in

$$\lambda = \Lambda_\lambda^{-1}(-J_\lambda M^{-1}(H + J_u^T u) - \dot{J}_\lambda \dot{q} + \ddot{r}_\lambda) \tag{5}$$

where $\Lambda_\lambda = J_\lambda M^{-1} J_\lambda^T$ is defined as the constraint decoupling matrix. In this study, the fully-constrained or over-constrained situation will *not* be considered. Therefore, the sufficient condition of ($\mathrm{rank}(J_\lambda) = n_\lambda;\ n_q > n_\lambda$) is provided to make sure that the system is under-constrained. This condition also assures that Λ_λ is automatically invertible. By substituting constraint forces into Equation (1a), the state space dynamics could be obtained as

$$\dot{x} = \begin{bmatrix} \dot{q} \\ M^{-1}\Phi_\lambda H + M^{-1} J_\lambda^T \Lambda_\lambda^{-1}(-\dot{J}_\lambda \dot{q} + \ddot{r}_\lambda) \\ J_\xi \dot{q} + \Omega_\xi \end{bmatrix} + \begin{bmatrix} 0 \\ M^{-1}\Phi_\lambda J_u^T \\ 0 \end{bmatrix} u \tag{6}$$

where $x = [q^T \ \dot{q}^T \ \xi^T]^T$ is the state vector and $\Phi_\lambda = (I_{n_q} - J_\lambda^T \Lambda_\lambda^{-1} J_\lambda M^{-1})$ is defined as the mapper that maps the system from the unconstrained manifold to the constrained manifold. A specific example of an MRS system with constraints and nonholonomic states will be provided later in Section 4, where the modelling of the aerial manipulator previously presented in Figure 1 will be explained in detail.

To control this system, the frequently used MBC approach is to design output functions such that the system is driven onto the desired manifold. As the system has n_q generalised coordinates and n_u actuator inputs, a set of control outputs, $y \in \mathbb{R}^{n_y}$ and its time derivatives, can be defined according to Equation (7). The output function $h : \mathbb{R}^{2n_q + n_\xi} \to \mathbb{R}^{n_y}$ is a class $\mathcal{C}^2$ function, and $\Omega_h \in \mathbb{R}^{n_y}$ is the remaining nonlinear term of q and ξ. The restriction on h ($n_y \leq \min(n_u, n_q - n_\lambda)$) is a necessary condition for the outputs to be controllable.

$$y = h(x); \quad \dot{y} = J_h(q, \xi)\dot{q} + \Omega_h(q, \xi); \quad \ddot{y} = J_h \ddot{q} + \dot{J}_h \dot{q} + \dot{\Omega}_h \tag{7}$$

With defining $r_h(t, x) : \mathbb{R}_+ \times \mathbb{R}^{2n_q + n_\xi} \to \mathbb{R}^{n_y}$ as the reference function for y, the output dynamics is

$$\begin{aligned} &\ddot{r}_h - \dot{J}_h \dot{q} - \dot{\Omega}_h \\ &\quad = J_h M^{-1}\Phi_\lambda H + J_h M^{-1}\Phi_\lambda J_u^T u + J_h M^{-1} J_\lambda^T \Lambda_\lambda^{-1}(\ddot{r}_\lambda - \dot{J}_\lambda \dot{q}) \end{aligned} \tag{8}$$

Therefore, the control effort is derived in Equation (9a) with the feed-forward controller u_f and feedback controllers u_b defined in Equations (9b) and (9c), respectively.

$$u = u_f + u_b \tag{9a}$$

$$\begin{aligned} u_f = \Lambda_u^\dagger \big[&(\ddot{r}_h - \dot{J}_h \dot{q} - \dot{\Omega}_h) \\ &- J_h M^{-1}\big(\Phi_\lambda H + J_\lambda^T \Lambda_\lambda^{-1}(\ddot{r}_\lambda - \dot{J}_\lambda \dot{q})\big)\big] \end{aligned} \tag{9b}$$

$$u_b = \Lambda_u^\dagger \psi(t, y, r_h) \tag{9c}$$

where $\Lambda_u^\dagger = O^{-\frac{1}{2}}(\Lambda_u O^{-\frac{1}{2}})^+$ is the weighted Moore-Penrose inverse term for the input decoupling matrix $\Lambda_u = J_h M^{-1}\Phi_\lambda J_u^T$, with the requirement of $\mathrm{rank}(\Lambda_u) = n_y$. $O \in \mathbb{R}^{n_u \times n_u}$ (Righetti et al., 2011) is a symmetric positive definite matrix. Apparently, $\Lambda_u^\dagger = \Lambda_u^{-1}$ for $n_y = n_u$. Function ψ can be designed according to the applied control scheme, e.g. a commonly used PD controller

$$u_{PD} = \Lambda_u^\dagger \psi_{PD} = \Lambda_u^\dagger \big(K_P(r_h - y) + K_D(\dot{r}_h - \dot{y})\big) \tag{10}$$

2.2 Robust adaptive control via inverse optimality

Although the MBC works well in theory, it ignores the model uncertainties as well as the external disturbances, both of which are frequently encountered in practice. Therefore, a robust adaptive controller with inverse optimality was proposed. Consider a system that contains model inaccuracy and disturbance, as in the following form

$$\dot{x}(t) = f(x) + g(x)u + F(x)\theta + G(x)w \tag{11}$$

where $x \in \mathbb{R}^{n_x}$ is the state vector, $u \in \mathbb{R}^{n_u}$ is the input vector, $\theta \in \mathbb{R}^{n_\theta}$ is the constant uncertainty parameter vector, and $w \in \mathbb{R}^{n_w}$ is the disturbance vector.

Definition 2.1 (Krstic & Deng, 1998; Krstic & Li, 1998; Luo et al., 2005)**:** For the system in Equation (11), a smooth function $V(x, \theta) : \mathbb{R}^{n_x} \times \mathbb{R}^{n_\theta} \to \mathbb{R}_+$ is a *robust adaptive control Lyapunov function*, if there exists a function $\alpha(x, \theta)$ smooth on $\{\mathbb{R}^{n_x} \backslash \{0\}\} \times \mathbb{R}^{n_\theta}$ that satisfies $\alpha(0, \theta) \equiv 0$, a continuous function $Q(x, \theta) : \mathbb{R}^{n_x} \times \mathbb{R}^{n_\theta} \to \mathbb{R}_+$, and a matrix $\Gamma = \Gamma^T > 0$ so that the control law $u = \alpha(x, \theta)$ satisfies

$$\frac{\partial V}{\partial x}\left(f + gu + F\left(\theta + \Gamma\left(\frac{\partial V}{\partial \theta}\right)^T\right)\right.$$

$$+ G\ell_\gamma(2\|\mathrm{L}_G V\|)\frac{(\mathrm{L}_G V)^T}{\|\mathrm{L}_G V\|^2}\Bigg) \le -Q(x,\theta) \tag{12}$$

for the auxiliary control system of

$$\dot{x} = f + gu + F\left(\theta + \Gamma\left(\frac{\partial V}{\partial \theta}\right)^T\right) + G\ell_\gamma(2\|\mathrm{L}_G V\|)\frac{(\mathrm{L}_G V)^T}{\|\mathrm{L}_G V\|^2} \tag{13}$$

where $\gamma(\sigma)$ is a class $\mathcal{K}_\infty$ function whose derivative $\gamma'(\sigma) = \partial\gamma/\partial\sigma$ is also a class $\mathcal{K}_\infty$ function. The function $\ell_\gamma(\sigma)$ denotes the Legendre-Fenchel transformation of $\ell_\gamma(\sigma) = \sigma(\gamma')^{-1}(\sigma) - \gamma((\gamma')^{-1}(\sigma)) = \int_0^\sigma (\gamma')^{-1}(s)\,\mathrm{d}s$.

Remark 2.1 (Krstic & Deng, 1998; Krstic & Li, 1998; Luo et al., 2005)**:** It has been shown that $F = 0$ will lead to the definition of *robust control Lyapunov function* (RCLF), and $G = 0$ will lead to the definition of *adaptive control Lyapunov function* (ACLF), respectively. Definition 2.1 is a consensus of both theories.

In addition to the definition of RACLF, the solvability of the adaptive control problem is also revisited. It is provided that the estimation of θ is $\hat{\theta}(t)$, and the estimation error is $\tilde{\theta} = \hat{\theta} - \theta$.

Definition 2.2 (Krstic & Deng, 1998; Luo et al., 2005)**:** The *adaptive control problem* of the system in Equation (11) is *solvable*, if there exists a function $\alpha(x,\hat{\theta})$ smooth on $\{\mathbb{R}^{n_x}\backslash\{0\}\} \times \mathbb{R}^{n_\theta}$ and satisfies $\alpha(0,\hat{\theta}) \equiv 0$, a smooth function $\beta(x,\hat{\theta}) : \mathbb{R}^{n_x} \times \mathbb{R}^{n_\theta} \to \mathbb{R}^{n_\theta \times n_\theta}$, and a matrix $\Gamma = \Gamma^T > 0$ such that

$$u = \alpha(x,\hat{\theta}); \quad \dot{\hat{\theta}} = \Gamma^{-1}\beta(x,\hat{\theta}) \tag{14}$$

guarantees the global boundedness of the tuple $(x,\hat{\theta})$, and asymptotic convergence of x, for all $\theta \in \mathbb{R}^{n_\theta}$.

If $V_0(x,\theta)$ is proven to be a RACLF together with the stabilising controller as $u = \alpha(x,\theta)$ for the auxiliary system in Equation (13), the control law in Definition 2.2 will asymptotically stabilise the system in Equation (11) with respect to the newly constructed Lyapunov function $V_1 = V_0 + (1/2)\tilde{\theta}^T\Gamma\tilde{\theta}$ (Krstic & Deng, 1998). Based on this result, the theorem of inverse optimal robust adaptive control can be established.

Theorem 2.1 (Luo et al., 2005)**:** *Based on the condition in Definitions* 2.1 *and* 2.2*, if there exists a function $R(x,\theta)$ that satisfies $R = R^T > 0$ so that the control law*

$$u = \alpha_0(x,\theta) = -R(x,\theta)^{-1}(\mathrm{L}_g V)^T \tag{15}$$

globally asymptotically stabilises Equation (13) *with respect to $V(x,\theta)$, then, the adaptive control law*

$$u = \alpha(x,\hat{\theta}) = -c_1 R(x,\hat{\theta})^{-1}(\mathrm{L}_g V)^T;$$
$$\dot{\hat{\theta}} = \Gamma^{-1}\beta(x,\hat{\theta}) = \Gamma^{-1}(\mathrm{L}_F V)^T \tag{16}$$

with $c_1 \ge 2$, solves the inverse optimal H_∞ adaptive control problem for the system described in Equation (11) *by minimising the cost function*

$$J_\alpha(u) = \sup_{w\in\mathbb{W}}\left\{\lim_{t\to\infty}\left[c_1\tilde{\theta}^T\Gamma\tilde{\theta} + 2c_1 V(x,\hat{\theta}) + \int_0^t \left(l(x,\hat{\theta}) + u^T R(x,\hat{\theta})u - c_1 c_2\gamma\left(\frac{\|w\|}{c_2}\right)\right)\mathrm{d}t\right]\right\} \tag{17}$$

for any $c_2 \in (0,2]$, where

$$l(x,\hat{\theta}) = -2c_1\mathrm{L}_f V - 2c_1\mathrm{L}_F V\left(\hat{\theta} + \Gamma\left(\frac{\partial V}{\partial\hat{\theta}}\right)^T\right) - c_1 c_2\ell_\gamma(2\|\mathrm{L}_G V\|) + c_1^2\mathrm{L}_g V R^{-1}(\mathrm{L}_g V)^T \tag{18}$$

and $\mathbb{W}$ is the set of locally bounded functions of x.

Remark 2.2 (Luo et al., 2005)**:** Similar to Remark 1, by assuming the parameter θ is known and setting $\Gamma = 0$, the inverse optimal robust control in Equation (15)–(18) yields the RCLF control law and its corresponding cost function. By setting $w = 0$, the ACLF controller that minimises its cost function can be acquired. As the two components of the RACLF, the two control laws are not coupled and can be applied separately.

2.3 Problem statement

The above theorems provide an effective way to design the controller to address model uncertainties and disturbance. However, it cannot be applied directly to the previously discussed MRS due to the unique *nonholonomic*, *under-actuated*, and *constrained* features. Therefore, the core of this work is to extend the above theories to the nonholonomically constrained modular robotic system, which has the following dynamics

$$\dot{x} = \begin{bmatrix} \dot{q} \\ M^{-1}(H + J_\lambda^T\lambda) \\ J_\xi\dot{q} + \Omega_\xi \end{bmatrix} + \begin{bmatrix} 0 \\ M^{-1}J_u^T \\ 0 \end{bmatrix} u + \begin{bmatrix} 0 \\ M^{-1}f_\theta \\ 0 \end{bmatrix} + \begin{bmatrix} 0 \\ M^{-1}f_w \\ 0 \end{bmatrix}; \tag{19}$$

where $f_\theta \in \mathbb{R}^{n_q}$ is the model uncertainty and $f_w \in \mathbb{R}^{n_q}$ is the disturbance. For this study, the output of the system is assumed to be undisturbed, which remains as Equation (7). It should be noted that f_θ and f_w will indirectly affect ξ and $\dot{q}$, since ξ and $\dot{q}$ are integrated from $\ddot{q}$. In this case, any uncertainties and disturbances affecting ξ and $\dot{q}$ can be included in f_θ and f_w. It should also be noted that the constraint uncertainties or disturbances are not considered, since any inaccuracy in the kinematic constraints can always be represented alternatively in the state equations. Under these conditions, the original controller may not be able to assure system convergence towards the desired trajectory. The controller may not even be able to stabilise the system if the uncertainties and disturbances are large.

3. Robust adaptive control solutions

To solve the formulated problem, adaptive control is studied first with the assumption $f_w = 0$. The robustness is then added through specific CLF design.

3.1 Adaptive control and model uncertainty assumptions

To formulate the adpative control law with $f_w = 0$, the error vector is defined as

$$e = \begin{bmatrix} e_I \\ e_P \\ e_D \end{bmatrix} = \begin{bmatrix} \int (y - r_h)\,\mathrm{d}t \\ y - r_h \\ \dot{y} - \dot{r}_h \end{bmatrix} \tag{20}$$

where e_I is the integral error. To limit the scope of the study, some reasonable assumptions (Luo et al., 2005) are made as follows

(S1) f_θ has the structure of

$$f_\theta = Y(x)\theta + L^\star(q,\xi,\theta)\ddot{q} \tag{21}$$

where $Y : \mathbb{R}^{2n_q+n_\xi} \to \mathbb{R}^{n_q \times n_\theta}$ is the state uncertainty regressor function of class $\mathcal{C}_\infty$ and $L^\star : \mathbb{R}^{n_q} \times \mathbb{R}^{n_\xi} \times \mathbb{R}^{n_\theta} \to \mathbb{R}^{n_q \times n_q}$ is the acceleration uncertainty map of class $\mathcal{C}_\infty$ that satisfies $L^\star(q,\epsilon,0) = 0$.

(S2) There exists a class $\mathcal{C}_\infty$ regressor function $L(q,\xi,\ddot{q}) : \mathbb{R}^{2n_q+n_\xi} \times \mathbb{R}^{n_q} \to \mathbb{R}^{n_q \times n_\theta}$, so that $L^\star(q,\xi,\theta)\ddot{q}$ satisfies

$$L^\star(q,\xi,\theta)\ddot{q} = L(q,\xi,\ddot{q})\theta \tag{22}$$

Here, (S1) is made based on the achievable setup that all of the states are measured with sensors. The structure demonstrates the existence of uncertainties from the force and inertia, which covers a wide variety of uncertainty sources. For (S2), the relationship in Equation (22) indicates the jointly affine property of the term $L^\star(q,\xi,\theta)\ddot{q}$ in the tuple $(\theta,\ddot{q})$.

Furthermore, for the input-output control problem where $J_h \neq I_{n_q}$, a conversion between $\ddot{q}$ and the output $\ddot{y}$ is required (Gu & Xu, 1995). It is possible to select the internal states of the control system as $q_i \in \mathbb{R}^{n_q - n_y}$ based on an nth rank permutation matrix S such that

$$\begin{bmatrix} \ddot{y} - \dot{J}_h\dot{q} - \dot{\Omega}_h \\ \ddot{q}_i \end{bmatrix} = \begin{bmatrix} J_h S^{-1} \\ \begin{bmatrix} 0 & I_{(n-n_y)\times(n-n_y)} \end{bmatrix} \end{bmatrix} S\ddot{q} = J_s S\ddot{q}; \tag{23}$$

Since the acceleration of the output tracking error is $\dot{e}_D = \ddot{y} - \ddot{r}_h = J_h\ddot{q} + \dot{J}_h\dot{q} + \dot{\Omega}_h - \ddot{r}_h$, the term y can be represented with $\dot{e}_D$ and $\ddot{r}_h$. Therefore, the term $L(x,\ddot{q})\theta$ can be equivalently converted to

$$L(x,\ddot{q})\theta = L_o(x,\dot{e}_D)\theta + L_i(x,\ddot{r}_h,\ddot{q}_i)\theta \tag{24}$$

where L_o and L_i are defined as

$$L_o(x,\dot{e}_D) = L\left(x, (J_s S)^{-1}\begin{bmatrix} \dot{e}_D^T & 0_{(n_q-n_y)\times 1}^T \end{bmatrix}^T\right); \tag{25a}$$

$$L_i(x,\ddot{r}_h,\ddot{q}_i) = L\left(x, (J_s S)^{-1}\begin{bmatrix} (\ddot{r}_h - \dot{J}_h\dot{q} - \dot{\Omega}_h)^T & \ddot{q}_i^T \end{bmatrix}^T\right). \tag{25b}$$

Base on the setup, provided that the estimation of θ is $\hat{\theta}(t) \in \mathbb{R}^{n_\theta}$, by adopting the feed-forward controller shown in Equation (9b) and the feedback controller as $u_b = \Lambda_u^\dagger \psi(x,e,\ddot{q}_i,\hat{\theta})$, the error dynamics becomes

$$\dot{e}_D = J_h M^{-1}\Phi_\lambda(Y(x)\theta + L_o(x,\dot{e}_D)\theta + L_i(x,\ddot{r}_h,\ddot{q}_i)\theta) + \psi \tag{26}$$

Therefore, the final error dynamics is obtained as

$$\dot{e} = \begin{bmatrix} 0 & I_{n_y} & 0 \\ 0 & 0 & I_{n_y} \\ 0 & 0 & 0 \end{bmatrix} e + \begin{bmatrix} 0 \\ 0 \\ J_h M^{-1}\Phi_\lambda\big(Y(x) + L_i\big)\theta \end{bmatrix} + \begin{bmatrix} 0 \\ 0 \\ J_h M^{-1}\Phi_\lambda L_o\theta \end{bmatrix} + \begin{bmatrix} 0 \\ 0 \\ \psi \end{bmatrix} \tag{27}$$

Here, based on (S2), more intermediate terms could be defined as

$$L_o^\star(x,\theta)\dot{e}_D = L_o(x,\dot{e}_D)\theta \tag{28a}$$

$$L_1(x,\dot{e}_D)\theta = J_h M^{-1}\Phi_\lambda L_o^\star(x,\theta)\dot{e}_D \tag{28b}$$

$$L_1^\star(x,\theta)\dot{e}_D = L_1(x,\dot{e}_D)\theta \tag{28c}$$

$$F(x,\ddot{r}_h,\ddot{q}_i) = J_h M^{-1}\Phi_\lambda\big(Y(x) + L_i(x,\ddot{r}_h,\ddot{q}_i)\big) \tag{28d}$$

where $L_o^\star(x,0) = L_1^\star(x,0) = 0$. Therefore, the system can be rearranged so that the right hand side of the equation involves no more than a 2nd order derivative of the error.

$$\begin{bmatrix} I & 0 & 0 \\ 0 & I & 0 \\ 0 & 0 & I - L_1^\star \end{bmatrix}\dot{e} = \begin{bmatrix} 0 & I & 0 \\ 0 & 0 & I \\ 0 & 0 & 0 \end{bmatrix} e + \begin{bmatrix} 0 \\ 0 \\ F\theta \end{bmatrix} + \begin{bmatrix} 0 \\ 0 \\ \psi \end{bmatrix}; \tag{29}$$

As in Equation (29), which demonstrates the error state system, the term $L_1^\star$ will affect the complexity of the control problem. Omitting $L_1^\star$ will lead to the inability to estimate some of the inertial uncertainties in the system. The solution lies in analysing the adaptive control Lyapunov function. Referring to Definitions 2.1, 2.2, and Remark 2.1, an ACLF (under zero disturbance) candidate based on Equation (29) can be selected as

$$V_{1,0} = \frac{1}{2}e^T P_e e; \tag{30}$$

where $P_e \in \mathbb{R}^{3n_y} \times \mathbb{R}^{3n_y}$ is a constant symmetric positive definite matrix and $\tilde{\theta} = \hat{\theta} - \theta$ is the parameter estimation error. Similar to Equation (12), it is easy to see that the ACLF condition requires satisfying the auxiliary control problem of

$$\dot{e} = \begin{bmatrix} 0 & I & 0 \\ 0 & 0 & I \\ 0 & 0 & 0 \end{bmatrix} e + \begin{bmatrix} 0 \\ 0 \\ F\theta + L_1^\star\dot{e}_D \end{bmatrix} + \begin{bmatrix} 0 \\ 0 \\ \psi_{1,0} \end{bmatrix} \tag{31}$$

with the controller $\psi_{1,0}$. By assuming $\psi_{1,0}$ as

$$\psi_{1,0}(x,e,\theta) = -F\theta + (I - L_1^\star)\psi_{PID} \tag{32}$$

with ψ_{PID} is defined as

$$\psi_{PID}(e) = -(K_I e_I + K_P e_P + K_D e_D) \tag{33}$$

where K_I, K_P, and K_D are constant symmetric positive definite matrices, the auxiliary system becomes

$$\begin{bmatrix} I & 0 & 0 \\ 0 & I & 0 \\ 0 & 0 & I - L_1^\star \end{bmatrix}\dot{e}$$

$$= \begin{bmatrix} 0 & I & 0 \\ 0 & 0 & I \\ -(I - L_1^\star)K_I & -(I - L_1^\star)K_P & -(I - L_1^\star)K_D \end{bmatrix} e$$

which yields

$$L_1^\star \dot{e}_D = L_1^\star \psi_{PID} \tag{34}$$

Equation (34) is used to approximate the uncertain dynamics $L_1^\star \dot{e}_D \approx L_1^\star \psi_{PID}$. It should be noted that $L_1^\star$ can also be viewed as the adaptive gain-tuning parameter matrix for the PID controller. Thus, it can be concluded that Equation (30) is an ACLF candidate if the following requirement is satisfied

$$A^T P_e + P_e A < 0; \quad A = \begin{bmatrix} 0 & I & 0 \\ 0 & 0 & I \\ -K_I & -K_P & -K_D \end{bmatrix} \tag{35}$$

Proposition 3.1: *For the error control system in Equation* (29)*, with* $L_1^\star \dot{e}_D \approx L_1^\star \psi_{PID}$ *through Equation* (34)*, and the PID gains (i.e.* K_I*,* K_P*, and* K_D*) satisfying the condition in Equation* (35)*, the controller*

$$\psi_1(x, e, \ddot{q}_i, \hat{\theta}) = -(F(x, \ddot{r}_h, \ddot{q}_i) + L_1(x, \psi_{PID}))\hat{\theta} + \psi_{PID} \tag{36}$$

and the adaptive update law

$$\dot{\hat{\theta}}_1 = \Gamma^{-1}(F(x, \ddot{r}_h, \ddot{q}_i) + L_1(x, \psi_{PID}))^T \times (P_{e,ID}^T e_I + P_{e,PD}^T e_P + P_{e,D} e_D) \tag{37}$$

where $P_{e,ID}, P_{e,PD}, P_{e,D} \in \mathbb{R}^{n_y} \times \mathbb{R}^{n_y}$ *are components of*

$$P_e = \begin{bmatrix} P_{e,I} & P_{e,PI} & P_{e,ID} \\ P_{e,PI}^T & P_{e,P} & P_{e,PD} \\ P_{e,ID}^T & P_{e,PD}^T & P_{e,D} \end{bmatrix}$$

will lead to the asymptotic stabilisation of the system with respect to the full Lyapunov function

$$V_1 = \frac{1}{2} e^T P_e e + \frac{1}{2} \tilde{\theta}^T \Gamma \tilde{\theta}; \tag{38}$$

Proof: Based on Equation (28c), by substituting the controller from Equation (36) into Equation (29), the error dynamics becomes (recall $\tilde{\theta} = \hat{\theta} - \theta$)

$$\dot{e} = \begin{bmatrix} 0 & I & 0 \\ 0 & 0 & I \\ 0 & 0 & 0 \end{bmatrix} e - \begin{bmatrix} 0 \\ 0 \\ F\tilde{\theta} - L_1^\star(x, \theta)\dot{e}_D + L_1^\star(x, \hat{\theta})\psi_{PID} \end{bmatrix} + \begin{bmatrix} 0 \\ 0 \\ \psi_{PID} \end{bmatrix} \tag{39}$$

with $L_1^\star(x, \hat{\theta})\dot{e}_D \approx L_1^\star(x, \hat{\theta})\psi_{PID}$ based on Equation (34), the above equation is further simplified as

$$\dot{e} = Ae - \begin{bmatrix} 0 \\ 0 \\ (F + L_1(x, \dot{e}_D))\tilde{\theta} \end{bmatrix} \tag{40}$$

Differentiating the Lyapunov function yields

$$\dot{V}_1 = \frac{1}{2}\dot{e}^T P_e e + \frac{1}{2} e^T P_e \dot{e} + \frac{1}{2}\dot{\tilde{\theta}}^T \Gamma \tilde{\theta} + \frac{1}{2}\tilde{\theta}^T \Gamma \dot{\tilde{\theta}} \tag{41}$$

Substituting the error dynamics from Equation (40) and the parameter update dynamics from Equations (37), (41) becomes

$$\begin{aligned} \dot{V}_1 &= \frac{1}{2} e^T (A^T P_e + P_e A) e - \begin{bmatrix} 0 & 0 & \tilde{\theta}^T (F + L_1)^T \end{bmatrix} P_e e \\ &\quad + \tilde{\theta}^T (F + L_1)^T (P_{e,ID}^T e_I + P_{e,PD}^T e_P + P_{e,D}^T e_D) \\ &= \frac{1}{2} e^T (A^T P_e + P_e A) e < 0 \end{aligned} \tag{42}$$

■

Remark 3.1: An understatement for the stability of the adaptive controller in Proposition 3.1 is the boundedness of $\dot{e}_D$ (Dawson et al., 1991; Spong & Ortega, 1990; H. Wang, 2011). From Equations (28c) and (40), it is obtained that

$$\left(I + L_1^\star(x, \hat{\theta}) - L_1^\star(x, \theta)\right)\dot{e}_D = -F\tilde{\theta} + \psi_{PID} \tag{43}$$

This is an indication that the boundedness of $\dot{e}_D$ is provided by the invertibility of $(I + L_1^\star(x, \hat{\theta}) - L_1^\star(x, \theta))$, which involves the estimated inertia uncertainty. From Equation (28), it can be recognised that $L_1^\star$ has the same unit dimension as the ratio between inertia matrices; with J_h as a kinematic term, $M^{-1}\phi_\lambda L_o^\star$ is comparable to the ratio between the modelled inertia M and inertia uncertain $L_o^\star$ mapped on the constrained manifold by ϕ_λ. Therefore, similar to the case discussed in Dawson et al. (1991), the existence of $(I + L_1^\star(x, \hat{\theta}) - L_1^\star(x, \theta))^{-1}$ may be ensured by reasonable adjusting M, the proposed controller has limitations in the applications where $L_o^\star$ is significant compared to M.

Remark 3.2: Another important condition for the adaptive controller is the availability of acceleration-related terms $L_1^\star \dot{e}_D$ and $\ddot{q}_i$. Since accelerations are affected by system inputs, the closed-form solution for these terms may not be available (Gu & Xu, 1995). In some cases where the knowledge of the system is available, $L_1^\star \dot{e}_D$ and $\ddot{q}_i$ may be estimated by forces and control inputs through the expression of e and x (as in the case of this study). This strategy, however, has limitations in the presence of significant model uncertainties and disturbances. It is also possible to acquire $L_1^\star \dot{e}_D$ and $\ddot{q}_i$ through acceleration measurement (Dawson et al., 1991; Ortega & Spong, 1989; Spong & Ortega, 1990) or filtering (H. Wang, 2011). For adaptive control stability, controllers designed using acceleration measurements can only be applied to limited scenarios where high precision measurement is available.

3.2 Robust adaptive CLF design

A detailed process of robust adaptive controller design can now be explained. Similarly, as there may be different sources where the disturbances originate, assumptions are made to limit the scope of the study, which are listed below

(S3) f_w has the structure of $f_w = c_2 W(x) w$ (Ghorbel et al., 1998) where $c_2 > 0$ is the disturbance magnitude parameter; $W : \mathbb{R}^{2n_q+n_\xi} \to \mathbb{R}^{n_q \times n_w}$ is the disturbance mapper of class $\mathcal{C}_\infty$; and $w \in \mathbb{R}^{n_w}$ is the disturbance vector.

(S4) $I - L_1^\star$ is invertible and locally bounded in x for fixed θ (Ghorbel et al., 1998).

Assumption (S3) is made so that the disturbances are considered affine external inputs into the system, where $c_2 \in \mathbb{R}_+$ is the assumed sensitivity parameter. For (S4), recall from Remark 3.1 that $L_1^\star$ is comparable to the ratio between modelled inertia M and inertia uncertainty $L_o^\star$. An unbounded inertia ratio usually indicates significant modelling inaccuracy that is unlikely to be caused by model uncertainty, which makes it reasonable to assume that for any θ the ratio between the known and unknown inertia is bounded in x. The error control system that involves disturbance can then be established based on the above assumptions and Equation (29) as

$$\begin{bmatrix} I & 0 & 0 \\ 0 & I & 0 \\ 0 & 0 & I - L_1^\star \end{bmatrix} \dot{e} = \begin{bmatrix} 0 & I & 0 \\ 0 & 0 & I \\ 0 & 0 & 0 \end{bmatrix} e + \begin{bmatrix} 0 \\ 0 \\ F\theta + J_h M^{-1} \Phi_\lambda (c_2 W(x) w) + \psi \end{bmatrix} \tag{44}$$

From Equation (44), it can be recognised that $(I - L_1^\star)$ would affect the relative sensitivity of system error towards the disturbance. The coupling of uncertainty and disturbance will increase the complexity of the problem, especially as the positiveness of $(I - L_1^\star)$ is unknown. By adopting the same auxiliary controller $\psi_{1,0}$ as defined in Equation (32) and based on (S4), the equivalent $\dot{e}_D$ is now calculated as

$$\dot{e}_D = \psi_{PID} + (I - L_1^\star)^{-1} J_h M^{-1} \Phi_\lambda W w \tag{45}$$

As an essential process of the controller design, the selection of RACLF is explained. Similar to Equation (30), the structure of the RACLF is selected as

$$V_{2,0}(e) = \frac{1}{2} e^T P_e e \tag{46}$$

Here, P_e is a symmetric positive definite matrix redesigned as

$$P_e = \begin{bmatrix} (k_1^2 + k_2^2 + k_i^2) K^T K & (k_i k_p + k_2 k_3) K^T K & k_i K^T K \\ (k_i k_p + k_2 k_3) K^T K & (k_3^2 + k_p^2) K^T K & k_p K^T K \\ k_i K^T K & k_p K^T K & K^T K \end{bmatrix} \tag{47}$$

where $k = [k_i, k_p, k_1, k_2, k_3] \in \mathbb{R}_+^5$ are constant gain coefficients and $K \in \mathbb{R}^{n_y \times n_y}$ is constant and positive definite. Note that this design does not cover all the available Lyapunov equations. The design, however, offers a systematic way to design a variety of desired RACLFs. As a result, Equation (46) can also be represented as

$$\begin{aligned} V_{2,0} = {} & \frac{1}{2} k_1^2 e_I^T K^T K e_I + \frac{1}{2} (k_2 K e_I + k_3 K e_P)^T (k_2 K e_I + k_3 K e_P) \\ & + \frac{1}{2} (k_i K e_I + k_p K e_P + K e_D)^T (k_i K e_I + k_p K e_P + K e_D) \end{aligned} \tag{48}$$

By defining $\epsilon = k_i e_I + k_p e_P + e_D$, it can be obtained that

$$\begin{aligned} \dot{\epsilon} &= k_p(\epsilon - k_i e_I - k_p e_P) + k_i e_P \\ &\quad + (L_1^\star \dot{e}_D + F\theta + J_h M^{-1} \Phi_\lambda W w + \psi) \\ &= k_p(\epsilon - k_i e_I - k_p e_P) + k_i e_P \\ &\quad + (L_1^\star (\psi_{PID} + (I - L_1^\star)^{-1} J_h M^{-1} \Phi_\lambda W w) \\ &\quad + F\theta + J_h M^{-1} \Phi_\lambda W w + \psi) \\ &= k_p(\epsilon - k_i e_I - k_p e_P) + k_i e_P \\ &\quad + (L_1^\star \psi_{PID} + F\theta + (I - L_1^\star)^{-1} J_h M^{-1} \Phi_\lambda W w + \psi) \end{aligned} \tag{49}$$

with the equality of $(I + L_1^\star (I - L_1^\star)^{-1}) = (I - L_1^\star)^{-1}$ (Henderson & Searle, 1981). Again, based on (S4), a new term G is introduced such that

$$G = c_w J_h M^{-1} \Phi_\lambda W; \tag{50}$$

where $c_w \in \mathbb{R}_+$ satisfies $\|c_\omega\| \geq c_2 \max(\|(I - L_1^\star)^{-1}\|)$ in the local domain of x for the fixed θ, which provides

$$\max(\|Gw\|) \geq c_2 \max(\|(I - L_1^\star)^{-1} J_h M^{-1} \Phi_\lambda W w\|) \tag{51}$$

As such, Gw is used as a compromised alternative for $(I - L_1^\star)^{-1} J_h M^{-1} \Phi_\lambda W w$ in the following derivation.

Secondly, the relationship between the disturbance and the control state is assumed. Referring to Definition 2.1 and Remark 2.1, the class $\mathcal{K}_\infty$ function γ_ϵ for $\mathcal{L}_2$ disturbance attenuation (Luo et al., 2005) can be selected as

$$\gamma_\epsilon(\sigma) = \sigma^2; \tag{52}$$

According to Definition 2.1, it can be calculated that $\mathrm{L}_G V_{2,0} = \epsilon^T K^T K G$. The assumed disturbance with respect to the control state can then be obtained as

$$w_\epsilon = \ell_{\gamma_\epsilon}(2\|(K^T K G)^T \epsilon\|) \frac{(K^T K G)^T \epsilon}{\|(K^T K G)^T \epsilon\|^2} = (K^T K G)^T \epsilon \tag{53}$$

provided that the auxiliary controller $\psi(x, e, \theta)$ for the auxiliary system has the structure of

$$\begin{aligned} \psi_{PID} &= -R_\epsilon^{-1} (K^T K)^T \epsilon; \\ \psi_{2,0}(x, e, \theta) &= -F(x, \ddot{r}_h, \ddot{q}_i)\theta + (I - L_1^\star(x, \theta))\psi_{PID} \end{aligned} \tag{54}$$

where $R_\epsilon(x, e) : \mathbb{R}^{2n_q+n_\xi} \times \mathbb{R}^{3n_y} \to \mathbb{R}^{n_y \times n_y}$ is symmetric positive definite. This leads to the final form of the auxiliary system of

$$\dot{\epsilon} = k_p(\epsilon - k_i e_I - k_p e_P) + k_i e_P$$

$$+ (-R_\epsilon^{-1}(K^TK)^T + G(K^TKG)^T)\epsilon \tag{55}$$

Taking the time derivative of $V_{2,0}$ yields

$$\begin{aligned}\dot{V}_{2,0} &= \mathrm{L}_f V_{2,0} + \epsilon^T K^T K(-R_\epsilon^{-1}K^TK + GG^TK^TK)\epsilon \\ &= \alpha_1 e_I^T K^T K e_I + \alpha_2 e_I^T K^T K e_P + \alpha_3 e_P^T K^T K e_P \\ &\quad + \epsilon^T K^T K(\beta_1 e_I + \beta_2 e_P) \\ &\quad + \epsilon^T K^T K(k_p I_{n_y} - R_\epsilon^{-1}K^TK + GG^TK^TK)\epsilon\end{aligned}$$

where

$$\begin{aligned}\mathrm{L}_f V_{2,0} &= k_1^2 e_I^T K^T K e_P + (k_2 e_I + k_3 e_P)^T K^T K(k_2 e_P \\ &\quad + k_3(\epsilon - k_i e_I - k_p e_P)) \\ &\quad + k_p \epsilon^T K^T K\epsilon - \epsilon^T K^T K(k_p(k_i e_I + k_p e_P) - k_i e_P)\end{aligned}$$

and

$$\begin{aligned}&\alpha_1 = -k_i k_2 k_3; \quad \alpha_2 = k_1^2 + k_2^2 - k_i k_3^2 - k_p k_2 k_3; \\ &\alpha_3 = k_2 k_3 - k_p k_3^2; \quad \beta_1 = k_2 k_3 - k_i k_p; \quad \beta_2 = k_3^2 + k_i - k_p^2\end{aligned}$$

To guarantee the existence of a positive definite R_ϵ that satisfies $\dot{V}_{2,0} < 0$, additional sufficient design conditions are offered such that

$$\begin{aligned}&2a_3^2\beta_1\beta_2 + \alpha_2 = 0; \quad (1+a_1)a_3^2\beta_1^2 + \alpha_1 = 0; \\ &(1+a_2)a_3^2\beta_2^2 + \alpha_3 = 0\end{aligned}$$

Hence, the existence of $a = [a_1, a_2, a_3] \in \mathbb{R}_+^3$ determines the feasibility of the selected gain coefficients k. The compatible k can also be designed by assuming an optimisation problem with constraints on k and a coefficients.

Assuming a suitable pair of k and c are found, the Lyapunov function can be further simplified as

$$\begin{aligned}\dot{V}_{2,0} &= -a_1 a_3^2\beta_1^2 e_I^T K^T K e_I - a_2 a_3^2\beta_2^2 e_P^T K^T K e_P \\ &\quad - a_3^2(\beta_1 e_I + \beta_2 e_P)^T K^T K(\beta_1 e_I + \beta_2 e_P) \\ &\quad + \epsilon^T K^T K(\beta_1 e_I + \beta_2 e_P) \\ &\quad + \epsilon^T K^T K(k_p I_{n_y} - R_\epsilon^{-1}K^TK + GG^TK^TK)\epsilon\end{aligned} \tag{56}$$

which also provides the alternative presentation of $\mathrm{L}_f V_{2,0}$ as

$$\begin{aligned}\mathrm{L}_f V_{2,0} &= -a_1 a_3^2\beta_1^2 e_I^T K^T K e_I - a_2 a_3^2\beta_2^2 e_P^T K^T K e_P + k_p \epsilon^T K^T K\epsilon \\ &\quad - a_3^2(\beta_1 e_I + \beta_2 e_P)^T K^T K(\beta_1 e_I + \beta_2 e_P) \\ &\quad + \epsilon^T K^T K(\beta_1 e_I + \beta_2 e_P)\end{aligned}$$

Therefore, by selecting R_ϵ such that

$$R_\epsilon^{-1} = \left[GG^T + \left(k_p + 1/(a_3^2)\right)(K^TK)^{-1} + C_R\right] \tag{57}$$

where $C_R \in \mathbb{R}^{n_y \times n_y}$ is the additional symmetric positive definite magnitude matrix, the RACLF derivative yields

$$\begin{aligned}\dot{V}_{2,0} &= -a_1 a_3^2\beta_1^2 e_I^T K^T K e_I - a_2 a_3^2\beta_2^2 e_P^T K^T K e_P \\ &\quad - \epsilon^T K^T K C_R K^T K\epsilon - ((1/a_3)\epsilon - a_3(\beta_1 e_I + \beta_2 e_P))^T \\ &\quad \times K^T K((1/a_3)\epsilon - a_3(\beta_1 e_I + \beta_2 e_P)) < -Q\end{aligned} \tag{58}$$

with $Q(e, \hat{\theta}) : \mathbb{R}^{2n_y} \times \mathbb{R}^{n_\theta} \to \mathbb{R}_+$.

3.3 Main result

Based on these preparations, the theorem of the H_∞ robust adaptive controller is proposed, which is a conclusive result of the study. Under the appropriate conditions, the main result is applicable to under-actuated, constrained, and nonholonomic robotic systems. The result is also consistent with the motivation as it is suitable for MRS.

Theorem 3.1: *Based on the assumed conditions* (S1)–(S4), *with the approximation* $L_1^\star \dot{e}_D \approx L_1^\star \psi_{PID}$ *through Equation* (34) *the disturbance conversion in Equation* (51), ψ_{PID} *defined in Equation* (54), R_ϵ *defined in Equation* (57), $u_f(x, \ddot{r}_h)$ *defined in Equation* (9b), *and* ψ_2 *defined as*

$$\psi_2(x, e, \ddot{q}_i, \hat{\theta}) = (I - L_1^\star(x, \hat{\theta}))\psi_{PID} - F(x, \ddot{r}_h, \ddot{q}_i)\hat{\theta} \tag{59}$$

the RD2 input-output robust adaptive controller

$$u(x, e, \ddot{q}_i, \hat{\theta}) = u_f(x, \ddot{r}_h) + \Lambda_u^\dagger \psi_2(x, e, \ddot{q}_i, \hat{\theta}) \tag{60}$$

along with the update law

$$\dot{\hat{\theta}}_2 = \Gamma^{-1}\left[F(x, \ddot{r}_h, \ddot{q}_i) + L_1(x, \psi_{PID})\right]^T K^T K\epsilon \tag{61}$$

can solve the trajectory tracking problem for the disturbed dynamic system in Equation (19) *by asymptotically stabilising the Lyapunov function*

$$V_2(e, \hat{\theta}) = \frac{1}{2}(e^T P_e e + \tilde{\theta}^T \Gamma \tilde{\theta}) \tag{62}$$

and minimising the cost function

$$\begin{aligned}J_\epsilon(\psi_\epsilon) = \sup_{w \in \mathbb{W}_\epsilon} \Bigg\{ \lim_{t \to \infty} \Bigg[&c_1 \|\tilde{\theta}^T \Gamma \tilde{\theta}\| + 2c_1 V_{2,0}(x, e, \hat{\theta}) \\ &+ \int_0^t \left(l_\epsilon(x, e, \hat{\theta}) - c_1 \|w\|^2 + \psi_\epsilon^T R_\epsilon(x)\psi_\epsilon \right) \mathrm{d}\tau \Bigg] \Bigg\}\end{aligned} \tag{63}$$

where

$$\begin{aligned}\mathrm{L}_f V_2 &= \mathrm{L}_f V_{2,0} \\ l_\epsilon &= -2c_1 \mathrm{L}_f V_2 - c_1 \ell_{\gamma_\epsilon}\left(2\|(K^TKG)^T\epsilon\|\right) \\ &\quad + c_1^2 \epsilon^T K^T K R_\epsilon^{-1} K^T K\epsilon\end{aligned} \tag{64}$$

$$\psi_\epsilon = \left(I - L_1^\star(q, \xi, \hat{\theta})\right)^{-1}(\psi_2 + F\hat{\theta}) = c_1 \psi_{PID} \tag{65}$$

if it satisfies the conditions that $K > 0$, $C_R = C_R^T > 0$, $k > 0$, $a > 0$, $c_1 > 2$, $c_w > 0$, *and* $\mathbb{W}_\epsilon$ *is the set of locally bounded functions of* ϵ *according to Equation* (52).

The *proof* of this theorem can be found in Appendix. Detailed explanation of Theorem 3.1 is provided below.

Remark 3.3: Theorem 3.1 proved that Equation (60) is an optimal controller for the control problem in terms of ψ_ϵ. It should be noted that the controller, u, is not fully penalised by the cost function. However, since u_f, F, and $L_1^\star$ have a fixed form and are agnostic of the output or error vectors when the dynamic and

estimated uncertainty model is determined, ψ_ϵ is the only feedback component of the full controller that is optimisable by the cost function.

Remark 3.4: The controller can only ensure the robustness towards the compromised disturbance of Gw. In practice, the robust control performance towards $c_2(I - L_1^\star)^{-1} J_h M^{-1} \Phi_\lambda W w$ cannot be quantitatively analysed since $(I - L_1^\star)^{-1}$ is unknown. As $L_1^\star$ is comparable to the ratio between modelled and uncertain inertia in terms of the outputs (see previous explanation in Remark 3.1), the ideal application condition of the controller would be a model with small inertia uncertainty ($L_1^\star \sim 0$) that results in $(I - L_1^\star)^{-1} \sim I$, which decreases the difference between Gw and $c_2(I - L_1^\star)^{-1} J_h M^{-1} \Phi_\lambda W w$.

Remark 3.5: For the introduced RACLF design process, the selection of the coefficient set k and a is affected by the dynamics of the robotic system indirectly. The cost function for the selection of an ideal k and the corresponding a is decided by the desired control performance according to the resulting Lyapunov function. However, k and a are independent of any detailed properties of the system and are only used to tune the ratio between the P, I, and D gains, which are uniformly shaped by $K^T K$.

4. Simulation

This section validates the proposed control technique through a trajectory tracking control of a 3-DOF manipulator mounted on a quadcopter platform, as shown in Figure 1, which involves under-actuation and nonholonomic constraints at the same time. The simulation is conducted based on a MATLAB toolbox developed by the authors following Kane's method (Kane & Levinson, 1985; J. Wang et al., 2018).

4.1 System setup

The aerial manipulator model setup is shown in Figure 2(a), where the centre of mass (COM) of the UAV is located at its geometric centre. With the UAV and manipulator denoted as system 1 and system 2, respectively, the whole system can be modelled as

$$\begin{bmatrix} M_1 & 0 \\ 0 & M_2 \end{bmatrix} \begin{bmatrix} \ddot{q}_1 \\ \ddot{q}_2 \end{bmatrix} = \begin{bmatrix} H_1 \\ H_2 \end{bmatrix} + \begin{bmatrix} J_{u_f}^T & 0 \\ 0 & J_{u_\tau}^T \end{bmatrix} \begin{bmatrix} u_f \\ u_\tau \end{bmatrix} + \begin{bmatrix} f_{\theta_1} \\ f_{\theta_2} \end{bmatrix} + \begin{bmatrix} f_{w_1} \\ f_{w_2} \end{bmatrix} + J_\lambda^T \lambda \tag{66a}$$

$$\begin{bmatrix} \dot{\xi}_1 \\ \dot{\xi}_2 \end{bmatrix} = \begin{bmatrix} J_{\xi_1} & 0 \\ 0 & J_{\xi_2} \end{bmatrix} \begin{bmatrix} \dot{q}_1 \\ \dot{q}_2 \end{bmatrix} \tag{66b}$$

with the generalised velocities being $\dot{q}_1 = [\dot{\rho}_1^T \ \omega_1^T]^T$ and $\dot{q}_2 = [\dot{\rho}_2^T \ \omega_2^T \ \dot{\delta}_2^T]^T$. $\rho \in \mathbb{R}^3$ represents the base translation; $\omega \in \mathbb{R}^3$ is the base angular velocity; $\delta_2 \in \mathbb{R}^3$ is the manipulator joint angles; the nonholonomic states $\xi_1 \in \mathbb{R}^4$ and $\xi_2 \in \mathbb{R}^4$ are the quaternion coordinates of the UAV base and the manipulator base, respectively. As mentioned in Equation (2) from Section 2.1, these nonholonomic states are calculated as

$$\dot{\xi}_1 = 0.5 \left(\xi_1 \times \begin{bmatrix} 0 & \omega_1^T \end{bmatrix}^T \right); \quad \dot{\xi}_2 = 0.5 \left(\xi_2 \times \begin{bmatrix} 0 & \omega_2^T \end{bmatrix}^T \right) \tag{67}$$

$J_{\xi_1} \in \mathbb{R}^{4\times3}$ and $J_{\xi_2} \in \mathbb{R}^{4\times3}$ are the Jacobian matrices calculated from Equation (67); $u_f = [u_{f_1}, u_{f_2}, u_{f_3}, u_{f_4}] \in \mathbb{R}^4$ are the quadcopter rotor input (thrust forces, which is proportional to the thrusts by coefficient κ); and $u_\tau = [u_{\tau_1}, u_{\tau_2}, u_{\tau_3}] \in \mathbb{R}^3$ are the manipulator joint torques. In particular, J_{u_f} is defined as

$$J_{u_f} = \begin{bmatrix} J_{u_{f,T}}^T & J_{u_{f,R}}^T \end{bmatrix}^T; \quad J_{u_{f,T}} = [0_{4\times2} \quad 1_{4\times1}] \, T_R(\xi_1)^T \tag{68}$$

where $J_{u_{f,T}} \in \mathbb{R}^{4\times3}$ and $J_{u_{f,R}} \in \mathbb{R}^{4\times3}$ are the input Jacobian submatrices corresponding to the force and torque generated by u_f; and $T_R : \mathbb{R}^4 \to \mathbb{R}^{3\times3}$ is the rotation matrix calculated from ξ_1 (Fresk & Nikolakopoulos, 2013).

For the fixture between the UAV base and the manipulator (Fresk & Nikolakopoulos, 2013), the constraint equation is obtained as

$$r_{\lambda_\rho} = 0 = \rho_1 - \rho_2; \tag{69a}$$

$$r_{\lambda_\xi} = 0 = [0_{3\times1} \quad I_3] \, (\xi_1 \times \bar{\xi}_2) \tag{69b}$$

where $r_\lambda = [r_{\lambda_\rho}^T, r_{\lambda_\xi}^T]^T \in \mathbb{R}^6$. Here, $r_{\lambda_\rho} \in \mathbb{R}^3$ is the translational displacement constraint, and $r_{\lambda_\xi} \in \mathbb{R}^3$ is the quaternion-based rotation constraint. These two constraints fix the base

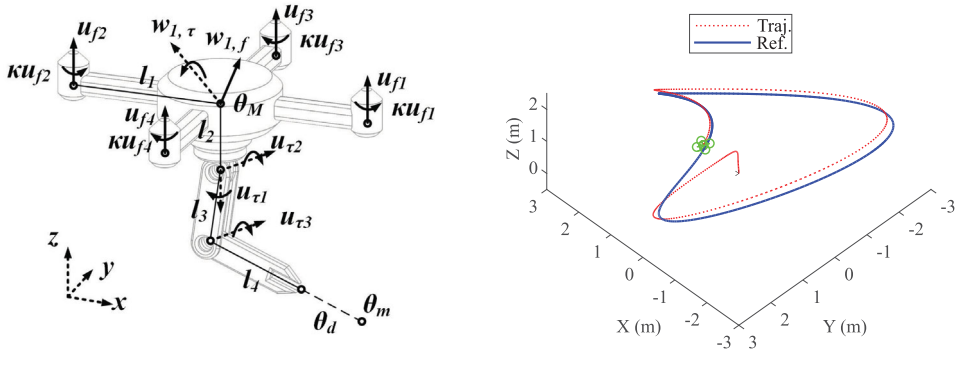

Figure 2. Simulation setups for the aerial manipulator case study. (a) Model information of aerial manipulator and (b) 3D view of trajectory and reference.

of the manipulator with the UAV in terms of translational displacements and rotations, respectively. The constraint Jacobian matrix $J_\lambda \in \mathbb{R}^{6\times 15}$ is calculated from r_λ. The Lagrange multiplier $\lambda \in \mathbb{R}^6$ calculated through Equation (5) is then applied as the constraint force to ensure that the coupling between the UAV and the manipulator systems satisfies Equation (69b). Therefore, the dynamical effects from the forces and torques experienced by one of the systems will pass to the other one through λ.

The uncertainties in this model were assumed to be the unknown point-mass θ_M attached on the COM of the UAV and an unknown point-mass θ_m of the payload with an unknown displacement θ_d along the final link of the arm. The uncertain payload effect could be also represented as an unknown point-mass θ_{m1} at the beginning of the final link, an unknown point-mass θ_{m2} at the tip of the final link, and an unknown moment θ_i along the radial direction of l_4. Therefore, the set of unknown properties was selected as $\theta = [\theta_M, \theta_{m_1}, \theta_{m_2}, \theta_i]^T \in \mathbb{R}^4$. In addition, the new parameters are uncoupled and affine in the system. The default uncertainty parameters were selected to have $\theta_m = 0.2$ kg and $\theta_d = 0.025$ m equivalently.

The system disturbances $w = [w_{1,f}^T, w_{1,\tau}^T, w_{2,\tau}^T]^T$ consist of the forces $w_{1,f} \in \mathbb{R}^3$ and torques $w_{1,\tau} \in \mathbb{R}^3$ acting on the UAV COM, and the torques $w_{2,\tau} \in \mathbb{R}^3$ acting on the manipulator joints. Thus, the disturbances are also affine to the system. Harmonic functions with different frequencies and amplitudes were used to design the disturbances

$$w_{1,f}(t) = (\sin(5t) + \sin(7.5t) + \sin(10t))(1_{3\times 1})$$
$$w_{1,\tau}(t) = 0.5(\sin(5t) + \sin(7.5t) + \sin(10t))(1_{3\times 1})$$
$$w_{2,\tau}(t) = 0.05(\sin(5t) + \sin(7.5t) + \sin(10t))(1_{3\times 1})$$

and the disturbance Jacobian matrix W was selected as

$$W_1 = \begin{bmatrix} I_3 & 0_{3\times 3} \\ 0_{3\times 3} & 0.5I_3 \end{bmatrix}; \quad W_2 = \begin{bmatrix} W_1 & 0_{6\times 3} \\ 0_{3\times 6} & 0.05I_3 \end{bmatrix};$$
$$W = \begin{bmatrix} W_1 & 0_{6\times 9} \\ 0_{9\times 6} & W_2 \end{bmatrix}^T$$

The reasoning for this selection was based on the analysis of $J_h M^{-1} \Phi_\lambda W$, which showed that δ_2 was most sensitive to the disturbances. Therefore, the selection of W should also ensure that the resulting control gain is not too large for the control frequency. All the standard parameters and properties are summarised in Table 2. To acquire accurate results, the simulation time step was set to 0.5×10^{-3} s. The control input and parameter update rates were set to 200 Hz. 40 N saturation is set for u_f. The selected k satisfied the CLF design condition.

The whole system control was realised with multi-loop control (Caccavale et al., 2014) that the position control loop calculates the desired attitude for tracking by estimating the thrust required for the system to follow a translational trajectory. It should be noted that the control scheme was established based on the assumption that the system response in attitude control is almost instantaneous when the moment of inertia of the system base is negligible compared to the control input capacity. The control output and control input for the two loops were selected as

$$y_1 = \begin{bmatrix} \rho_1^T & \delta_2^T \end{bmatrix}^T; \quad y_2 = \begin{bmatrix} ([0 \quad 0 \quad 1]\,\rho) & \delta_2^T & \xi_{err}^T \end{bmatrix}^T$$
$$u_1 = \begin{bmatrix} u_{v_f}^T & u_\tau^T \end{bmatrix}^T; \quad u_2 = \begin{bmatrix} u_f^T & u_\tau^T \end{bmatrix}^T;$$

where $\xi_{err} \in \mathbb{R}^3$ is the quaternion error calculated between the reference and state quaternion and $u_{v_f} \in \mathbb{R}^3$ is the virtual force acting at the COM of the UAV. The control framework will be applied to both loops, whereas $K_1 \in \mathbb{R}^{6\times 6}$ and $C_{R_1} \in \mathbb{R}^{6\times 6}$ were for the position loop control, while $K_2 \in \mathbb{R}^{7\times 7}$ and $C_{R_2} \in \mathbb{R}^{7\times 7}$ were for attitude loop control, respectively.

The 3D overview of the position trajectory is shown in Figure 2(b). The reference trajectory vectors are defined as

$$r_{h_1} = \begin{bmatrix} r_{h,\rho}^T & r_{h,\delta}^T \end{bmatrix}^T; \quad r_{h_2} = \begin{bmatrix} r_{h,z} & r_{h,\xi}^T & r_{h,\delta}^T \end{bmatrix}^T$$
$$r_{h,\xi} = \begin{bmatrix} r_{h,x} & r_{h,y} & r_{h,z} \end{bmatrix}^T; \quad r_{h,\xi} = \begin{bmatrix} r_{h,roll} & r_{h,pitch} & r_{h,yaw} \end{bmatrix}^T;$$
$$r_{h,\delta} = \begin{bmatrix} r_{h,\delta_1} & r_{h,\delta_2} & r_{h,\delta_3} \end{bmatrix}^T$$

for y_1 and y_2 in the two control loops respectively. The trajectories were designed as smooth periodic functions:

$$r_{h,x} = a_{A,1}(\cos(\omega_{c_1} t) - 0.5\sin(\omega_{c_2} t))$$
$$r_{h,y} = a_{A,1}(\sin(\omega_{c_1} t) - 0.5\sin(\omega_{c_2} t))$$
$$r_{h,z} = a_{A,2}\sin(\omega_{c_2} t); \quad r_{h,yaw} = \omega_{c_1} t; \quad r_{h,\delta_1} = \omega_{c_3} t$$
$$r_{h,\delta_2} = a_{A,1}\sin(\omega_{c_2} t); \quad r_{h,\delta_3} = a_{A,1}\sin(\omega_{c_2} t)$$

Here, $a_A = [a_{A,1}, a_{A,2}, a_{A,3}] \in \mathbb{R}_+^3$ are the amplitude coefficients and $\omega_c = [\omega_{c_1}, \omega_{c_2}, \omega_{c_3}] \in \mathbb{R}_+^3$ are the periodic rate coefficients. The attitude references $r_{h,roll}$ and $r_{h,pitch}$ are planned based on r_{yaw} and $u_{v,f}$ calculated from the outer control loop. The attitude references in Euler angles are then converted into the quaternion references for the inner control loop.

Based on the above information, the control flow chart is demonstrated in Figure 3. In the framework, $u_{f,1}$ and $u_{f,2}$ are the feed-forward controllers calculated for the outer and inner loops, respectively. Based on the simulation setup, the accelerations of internal states $\ddot{q}_i = [\ddot{\rho}_x, \ddot{\rho}_y]^T$ are required. While the system is under-actuated, $\ddot{\rho}_x$, $\ddot{\rho}_y$, and $\ddot{\rho}_z$ are interdependent provided that thrusts and the gravitational forces are the only external forces acting on the aerial manipulator. From Equations (66) and (68), by assuming the ideal condition that $w \sim 0$, the ratio between the translational accelerations can be calculated based on

$$(m_{\text{UAV}} + m_{\text{arm}} + \theta_M + \theta_{m_1} + \theta_{m_2}) \begin{bmatrix} \ddot{\rho}_x & \ddot{\rho}_y & \ddot{\rho}_z + c_G \end{bmatrix}^T$$

Table 2. Model and control parameter selections.

Prop.	Val.	Prop.	Val.
m_{UAV}	5 kg	m_{arm}	1.7 kg
θ	[2 kg, −0.0625 kg, 0.3125 kg, 7.815e−4 kg − m^2]	$a_{A,1}$	[2, 0.5, 1]
ω_c	[0.5, 1, 1.5]	k	[0.1, 0.75, 0.05, 0.05, 0.25]
c_w	0.1	c_1	2
C_{R_1}	$1.5I_6$	C_{R_2}	$1.5I_7$
K_1	diag([2, 2, 2, 2, 2, 2])$^{0.5}$	K_2	diag([2, 2, 2, 2, 3, 3, 3])$^{0.5}$
Γ	0.5diag([10^1, 10^2, 10^2, 10^5])	l	[0.15 m, 0.07 m, 0.075 m, 0.1 m]
κ	0.05	$x(0)$	$[0_{1\times 30}, 1, 0_{1\times 3}, 1, 0_{1\times 3}]^T$

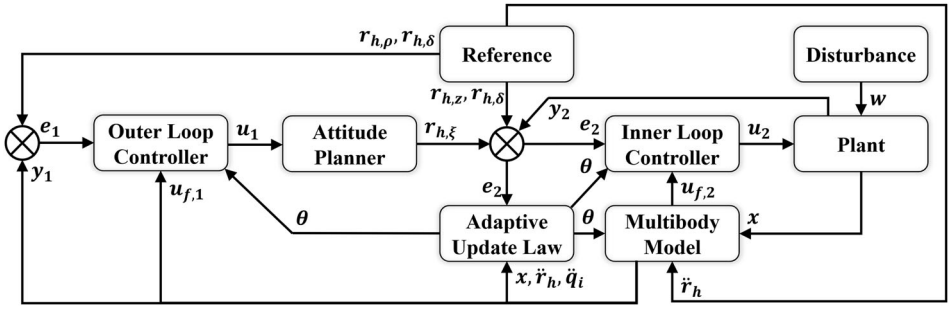

Figure 3. The multi-loop control framework of the aerial manipulator.

$$= J_{u_{f,T}}^{T} u_f \tag{70}$$

where c_G is the gravitational acceleration (9.81m/s^2). For estimation, similar to Equation (45), we can estimate $\ddot{\rho}_z = \ddot{r}_{h,z} + \dot{e}_{D,z}$, where $\dot{e}_{D,z}$ is the first element of the feedback acceleration $R_\epsilon^{-1} K^T K \epsilon$ in Equation (59) calculated from the outer control loop. Hence, based on the knowledge of the forces in the system (recall Remark 3.2), $\ddot{q}_i$ can be estimated based on the relationship in Equation (70).

4.2 Results and discussion

With the standard controller first implemented in the simulation, Figure 4 shows the comparison between position errors under zero-disturbance condition in the upper row, and under disturbance in the lower row. It should be noted that both sets of error did not converge to zero, as the steady state tracking errors oscillated periodically in both simulations. This may be as a result of a delayed response due to input rate limitation or the moment of inertia of the system floating base, which was assumed to be negligible during the controller design. The non-smooth attitude reference acquired from the outer control loop with numerical differentiation may also be a reason for the oscillations in the output errors.

The disturbance had a significant effect on the control performance as the amplitudes of the error oscillations were significantly larger. The result also showed that the joint angles δ_2 were greatly affected by the disturbances, which is likely due to the low inertia of the links near the end of the manipulator. However, under both conditions the controller managed to contain the system in the vicinity of the error equilibrium ($e = 0$). The control input for the disturbed system is shown in Figure 5, where it is apparent that the rotor input never exceeded 40 N. The joint motor input oscillates with magnitudes less than 2 N-m.

In these two simulations, the robustness augmentation part of the controller was already playing an effective role. To demonstrate the effect, the norm of the steady state errors from simulations with different control parameters were compared and analysed. In the subplots on the upper row of Figure 6, c_w was tuned to adjust the strength of the robustness augmentation of the controller. As the disturbances had the most significant effect on the joints, the robust control contributes the most to the disturbance attenuation in the manipulator joint angle errors. The result shows that doubling c_w greatly alleviates these errors, while it also slightly affected the performance in position and quaternion tracking. On the other hand, by decreasing c_w to 0, the controller was equivalent to an adaptive PID controller. In this case, the norm of the joint angle error had peaked over 0.5 rad, which was significantly higher than the errors in the simulations with robust control.

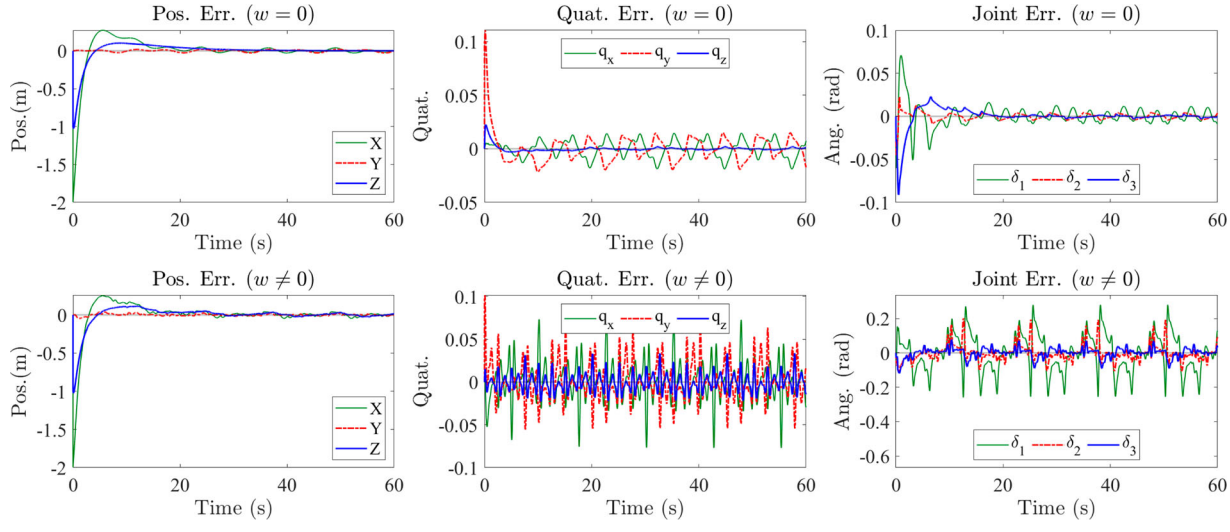

Figure 4. Comparison of position errors between zero-disturbance (upper row) and disturbed conditions (lower row).

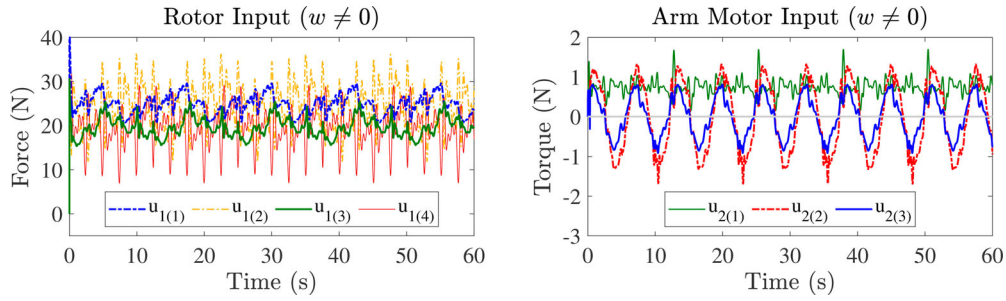

Figure 5. Control input of the system under disturbed simulation.

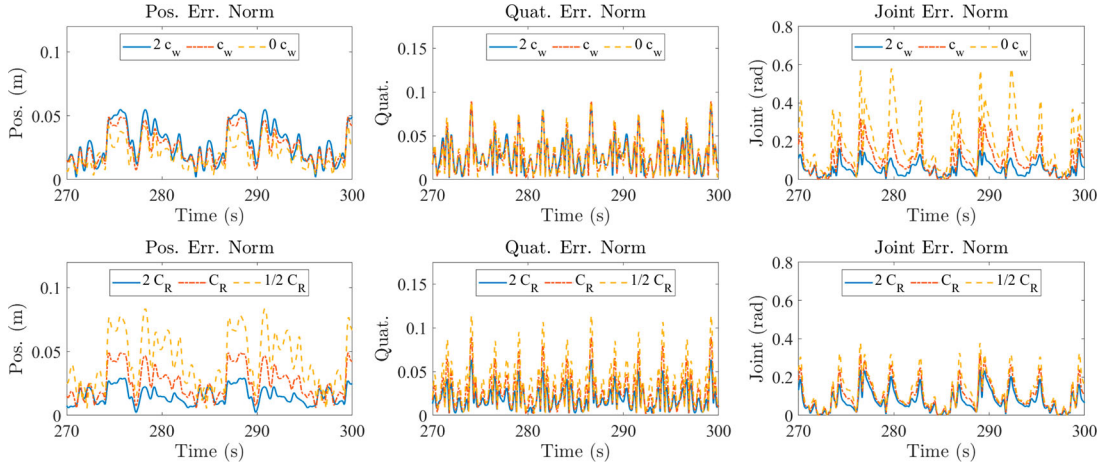

Figure 6. Performance comparison of controllers with different parameters (upper row: different c_w; lower row: different C_R) under disturbance.

The subplots on the lower row of Figure 6 compare the performance of controllers with a different performance parameter C_R. When C_R was increased, the error oscillation amplitudes recognisably decreased in position and quaternion tracking. Improving the control gain usually yields better performance and robustness, while a high control gain also requires higher input capacity in power and rate. It is also noticed that the performance improvement in reducing the joint angle errors was not as insignificant when compared with increasing c_w. The definition of G in Equation (50) implies the susceptibility of outputs with respect to the noise, which is determined by the disturbance magnitude indicated by W versus the inertia M. Therefore, increasing c_w is different from increasing C_R in the way that it can specifically target the most disturbance-sensitive outputs, which in this case are the manipulator joints. This also implies that a good estimation of W in practical applications is crucial toward the robustness of the controller design.

As shown in Figure 7, the uncertainty parameters in the two simulations did not converge to the true value. Apart from eliminating numerical errors, the perfect convergence of the parameters for this system requires reliable estimation of accelerations $\ddot{q}$, carefully selected adaptive gain Γ, and appropriate control input rates. In these simulations, the closed form presentation of $\ddot{q}$ cannot be acquired due to under-actuation. As mentioned previously in Section 4.1, the 2nd order derivative of the internal states $\ddot{q}_i$ was approximated from $\dot{e}_{D,z}$ and $\ddot{r}_{h,z}$. The approximation used $r_{h,\xi}$ to determine the ratio between the three translational accelerations, only considered the effect of the lifting thrust and gravitational force. Therefore, the delay in attitude tracking and the approximation error due to other model effects (e.g. air viscosity damping in the simulation) have caused the uncertainty parameter to oscillate in the vicinity of the true value. The subplots on the lower row show that the disturbance can worsen the convergence of the parameters. Increasing Γ will reduce the sensitivity of the uncertainty parameter dynamics towards the disturbances, while it also increases the time for it to reach steady state.

However, for fully-actuated or over-actuated systems, $\ddot{q}$ can be fully acquired based on estimating the $\dot{e}_d$ from Equation (31), which can result in better uncertainty parameter convergence. To demonstrate this feature, the setup for the original system was modified so that $u = [u_{v_f}^T, u_{v_\tau}^T, u_\tau^T]^T$ where the virtual torque $u_{v_\tau} \in \mathbb{R}^3$ shares the same input Jacobian as $w_{1,\tau}$, which leads to a fully-actuated system. This system was also assumed to be unperturbed with $w = 0$ and having a control input rate of 2000 Hz. In Figure 8, the errors between the true value and estimated uncertainty parameters of the fully actuated system at steady state are presented, where the time window has been zoomed to $t \in [300, 600]$ in seconds. It is clearly shown that the uncertainty parameters in a fully actuated system had a much better convergence, under the condition that the adopted model uncertainty structure f_θ in controller design match with the real application case.

Finally, it should be emphasised that the whole-body controller for this system was fully based on the individual dynamic properties from each module, as M, H, J_u, $L_1^\star$, F, and W can all be separately prepared. This shows that the basic goal of establishing a controller framework for a modular robotic system is

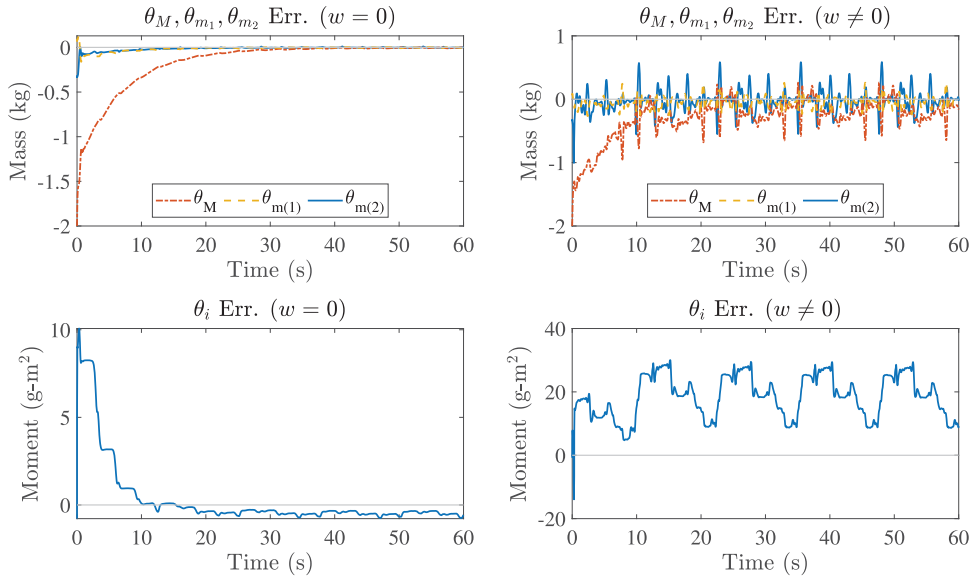

Figure 7. Comparison of uncertainty parameter error.

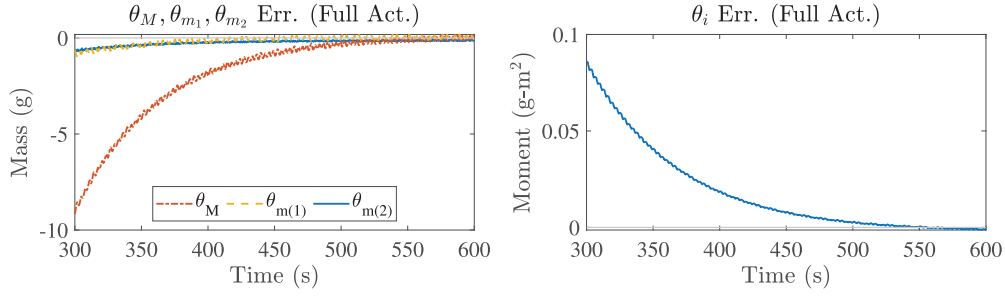

Figure 8. Adaptive parameter error of the fully actuated system simulation.

obtained. The simulation has verified the feasibility of the technique, and refining the performance will be a topic of interest for future work.

5. Conclusion and future work

This paper proposed a framework of robust adaptive input-output controller design for constrained and nonholonomic robotic systems. The adaptive model regression and gain tuning was realised by parameter affine model-based functions, and the H_∞ robustness augmentation was obtained based on inverse optimality. With reasonable application assumptions, the simulation results have corroborated the main theorem presented in the paper, which proves the feasibility of the framework by showing the error convergence, uncertainty parameters and the attenuation of disturbance effects. As a major objective, the control framework has realised a whole-body control of a robotic system completely established on the individual properties of the modules.

The control framework presented in this paper has a number of limitations that require attentions in future works. The proposed method can be further improved by (1) investigating approaches to avoid the use of estimations or measurements of acceleration-related terms; (2) exploring more flexible CLF design techniques to support a wider variety of control requirements; (3) extending the control framework to applications in switching and hybrid systems. The control framework should also be further studied on real applications, in which factors involving noise from sensors and discrete dynamic behaviours may occur. By the conclusion of the study, the developed theory can sufficiently provide a preliminary robust adaptive control template for a wide family of robots.

Disclosure statement

No potential conflict of interest was reported by the author(s).

ORCID

Yujiong Liu http://orcid.org/0000-0003-4926-5109
Pinhas Ben-Tzvi http://orcid.org/0000-0002-9452-482X

References

Aliyu, M. (2011). *Nonlinear H-infinity control, hamiltonian systems and hamilton-jacobi equations*. CRC Press.

Ames, A. D., Galloway, K., Sreenath, K., & Grizzle, J. W. (2014). Rapidly exponentially stabilizing control lyapunov functions and hybrid zero dynamics. *IEEE Transactions on Automatic Control*, *59*(4), 876–891. https://doi.org/10.1109/TAC.2014.2299335

Arimoto, S., Liu, Y. H., & Naniwa, T. (1993, May 2–6). Model-based adaptive hybrid control for geometrically constrained robots. In *Proceedings IEEE international conference on robotics and automation, Atlanta, GA, United States* (Vol. 1, pp. 618–623). IEEE.

Buschmann, T., Lohmeier, S., Ulbrich, H., & Pfeiffer, F. (2006, May 15–19). Dynamics simulation for a biped robot: Modeling and experimental verification. In *Proceedings 2006 IEEE international conference on robotics and automation, 2006 (ICRA2006), Orlando, FL, United States* (pp. 2673–2678). IEEE.

Caccavale, F., Giglio, G., Muscio, G., & Pierri, F. (2014). Adaptive control for UAVs equipped with a robotic arm. *IFAC Proceedings Volumes*, *47*(3), 11049–11054. https://doi.org/10.3182/20140824-6-ZA-1003.00790

Cloutier, J. R. (1997, June 6). State-dependent Riccati equation techniques: An overview. In *Proceedings of the 1997 American control conference, Albuquerque, NM, United States* (Vol. 2, pp. 932–936). IEEE.

Davey, J., Kwok, N., & Yim, M. (2012). Emulating self-reconfigurable robots-design of the SMORES system. In *2012 IEEE/RSJ international conference on intelligent robots and systems (IROS)* (pp. 4464–4469). IEEE.

Dawson, D., Lewis, F., Spong, M., & Ortega, R. (1991). Comments on "On adaptive inverse dynamics control of rigid robots" [with reply]. *IEEE Transactions on Automatic Control*, *36*(10), 1215–1216. https://doi.org/10.1109/9.90240

Freeman, R., & Kokotovic, P. V. (2008). *Robust nonlinear control design: State-space and lyapunov techniques*. Springer Science & Business Media.

Fresk, E., & Nikolakopoulos, G. (2013, July 17–19). Full quaternion based attitude control for a quadrotor. In *2013 European control conference (ECC), Zurich, Switzerland* (pp. 3864–3869). IEEE.

Ghorbel, F., Srinivasan, B., & Spong, M. W. (1998). On the uniform boundedness of the inertia matrix of serial robot manipulators. *Journal of Robotic Systems*, *15*(1), 17–28. https://doi.org/10.1002/(ISSN)1097-4563

Griffin, B., & Grizzle, J. (2017). Nonholonomic virtual constraints and gait optimization for robust walking control. *The International Journal of Robotics Research*, *36*(8), 895–922. https://doi.org/10.1177/0278364917708249

Gu, Y. L., & Xu, Y. (1995). A normal form augmentation approach to adaptive control of space robot systems. *Dynamics and Control*, *5*(3), 275–294. https://doi.org/10.1007/BF01968678

Guo, Y., & Woo, P. Y. (2003). An adaptive fuzzy sliding mode controller for robotic manipulators. *IEEE Transactions on Systems, Man, and Cybernetics-Part A: Systems and Humans*, *33*(2), 149–159.

Henderson, H. V., & Searle, S. R. (1981). On deriving the inverse of a sum of matrices. *SIAM Review*, *23*(1), 53–60. https://doi.org/10.1137/1023004

Kane, T. R., & Levinson, D. A. (1985). *Dynamics, theory and applications*. McGraw Hill.

Krstic, M., & Deng, H. (1998). *Stabilization of nonlinear uncertain systems*. Springer.

Krstic, M., & Li, Z. H. (1998). Inverse optimal design of input-to-state stabilizing nonlinear controllers. *IEEE Transactions on Automatic Control*, *43*(3), 336–350. https://doi.org/10.1109/9.661589

Kurdila, A. J., & Ben-Tzvi, P. (2019). *Dynamics and control of robotic systems*. John Wiley & Sons.

Lewis, F. L., Vrabie, D., & Syrmos, V. L. (2012). *Optimal control*. John Wiley & Sons.

Luo, W., Chu, Y. C., & Ling, K. V. (2005). Inverse optimal adaptive control for attitude tracking of spacecraft. *IEEE Transactions on Automatic Control*, *50*(11), 1639–1654. https://doi.org/10.1109/TAC.2005.858694

Melek, W. W., & Goldenberg, A. A. (2003, September). Neurofuzzy control of modular and reconfigurable robots. *IEEE/ASME Transactions on Mechatronics*, *8*(3), 381–389. https://doi.org/10.1109/TMECH.2003.816802

Moubarak, P., & Ben-Tzvi, P. (2012). Modular and reconfigurable mobile robotics. *Robotics and Autonomous Systems*, *60*(12), 1648–1663. https://doi.org/10.1016/j.robot.2012.09.002

Nguyen, K. D., & Dankowicz, H. (2015). Adaptive control of underactuated robots with unmodeled dynamics. *Robotics and Autonomous Systems*, *64*, 84–99. https://doi.org/10.1016/j.robot.2014.10.009

Nguyen, Q., & Sreenath, K. (2015). Optimal robust control for bipedal robots through control Lyapunov function based quadratic programs. In *Robotics: Science and systems*.

Ortega, R., & Spong, M. W. (1989). Adaptive motion control of rigid robots: A tutorial. *Automatica*, *25*(6), 877–888.

Peters, J., Vijayakumar, S., & Schaal, S. (2003, September 29–30). Reinforcement learning for humanoid robotics. In *Proceedings of the third IEEE-RAS international conference on humanoid robots, Karlsruhe-Munich, Germany* (pp. 1–20). IEEE.

Righetti, L., Buchli, J., Mistry, M., & Schaal, S.(2011, May 9–13). Inverse dynamics control of floating-base robots with external constraints: A unified view. In *2011 IEEE international conference on robotics and automation (ICRA), Shanghai, China* (pp. 1085–1090). IEEE.

Shah, S., Saha, S., & Dutt, J. (2012). Modular framework for dynamic modeling and analyses of legged robots. *Mechanism and Machine Theory*, *49*, 234–255. https://doi.org/10.1016/j.mechmachtheory.2011.10.006

Slotine, J. J. E., & Di Benedetto, M. (1990). Hamiltonian adaptive control of spacecraft. *IEEE Transactions on Automatic Control*, *35*(7), 848–852. https://doi.org/10.1109/9.57028

Slotine, J. J. E., & Li, W. (1987). On the adaptive control of robot manipulators. *The International Journal of Robotics Research*, *6*(3), 49–59. https://doi.org/10.1177/027836498700600303

Spong, M. W., & Ortega, R. (1990). On adaptive inverse dynamics control of rigid robots. *IEEE Transactions on Automatic Control*, *35*(1), 92–95. https://doi.org/10.1109/9.45152

Sugeno, M. (1985). An introductory survey of fuzzy control. *Information Sciences*, *36*(1–2), 59–83. https://doi.org/10.1016/0020-0255(85)90026-X

Wang, H. (2011). On adaptive inverse dynamics for free-floating space manipulators. *Robotics and Autonomous Systems*, *59*(10), 782–788. https://doi.org/10.1016/j.robot.2011.05.013

Wang, J., Kamidi, V. R., & Ben-Tzvi, P. (2018, September 30–October 3). A multibody toolbox for hybrid dynamic system modeling based on nonholonomic symbolic formalism. In *Dynamic systems and control conference, Atlanta, GA, United States* (Vol. 51913, p. V003T29A003). American Society of Mechanical Engineers.

Wei, H., Chen, Y., Tan, J., & Wang, T. (2011). Sambot: A self-assembly modular robot system. *IEEE/ASME Transactions on Mechatronics*, *16*(4), 745–757. https://doi.org/10.1109/TMECH.2010.2085009

Whitcomb, L. L., Arimoto, S., Naniwa, T., & Ozaki, F. (1997). Adaptive model-based hybrid control of geometrically constrained robot arms. *IEEE Transactions on Robotics and Automation*, *13*(1), 105–116. https://doi.org/10.1109/70.554351

Xin, M., & Balakrishnan, S. (2005). A new method for suboptimal control of a class of non-linear systems. *Optimal Control Applications and Methods*, *26*(2), 55–83. https://doi.org/10.1002/(ISSN)1099-1514

Yim, M., Shen, W., Salemi, B., Rus, D., Moll, M., Lipson, H., Klavins, E., & Chirikjian, G. S. (2007, March). Modular self-reconfigurable robot systems [grand challenges of robotics]. *IEEE Robotics & Automation Magazine*, *14*(1), 43–52. https://doi.org/10.1109/MRA.2007.339623

Yoon, H., & Tsiotras, P. (2008). Adaptive spacecraft attitude tracking control with actuator uncertainties. *The Journal of the Astronautical Sciences*, *56*(2), 251–268. https://doi.org/10.1007/BF03256551

Appendix. Proof of Theorem 3.1

With the equality of

$$\ell_{\gamma_\epsilon}\left(2\|(K^TKG)^T\epsilon\|\right) = \epsilon^T(K^TKG)(K^TKG)^T\epsilon$$

the derivative of Equation (62) can be presented in the form

$$\dot{V}_2(e,\hat{\theta}) = \mathrm{L}_f V_2 + \epsilon^T K^T K(F + L_1(x,\dot{e}_D))\theta + \epsilon^T K^T K\psi_{2,0}(x,e,\ddot{q}_i,\hat{\theta}) + \ell_{\gamma_\epsilon}\left(2\|(K^TKG)^T\epsilon\|\right) - \tilde{\theta}^T\Gamma\dot{\hat{\theta}}$$

with the previous setups of the feedback control law in Equation (54). According to Proposition 3.1, with the approximation $L_1^\star\dot{e}_D \approx L_1^\star\psi_{PID}$ through Equation (34), and provided that the parameter update law for $\psi_{2,0}$ is

$$\dot{\hat{\theta}}_{2,0} = \Gamma^{-1}\left(F + L_1(x,\psi_{PID})\right)^T K^T K\epsilon \tag{A1}$$

the $\dot{V}_2(x,e,\hat{\theta})$ term can be further simplified as

$$\begin{aligned}\dot{V}_2(e,\hat{\theta}) &= \mathrm{L}_f V_2 + \left(\epsilon^T K^T K(F + L_1(x,\psi_{PID}))\tilde{\theta} - \tilde{\theta}^T\Gamma\dot{\hat{\theta}}\right) \\ &\quad - \epsilon^T K^T K R_\epsilon^{-1} K^T K\epsilon + \ell_{\gamma_\epsilon}\left(2\|(K^TKG)^T\epsilon\|\right) \\ &= -\frac{1}{2c_1}\left(l_\epsilon - (c_1^2 - 2c_1)\epsilon^T K^T K R_\epsilon^{-1} K^T K\epsilon\right.\end{aligned}$$

$$
\begin{aligned}
&- c_1 \ell_{\gamma_\epsilon}\left(2\|(K^TKG)^T\epsilon\|\right)\Big) \\
&= \dot{V}_{2,0}(e) \leq -Q(e,\hat{\theta})
\end{aligned}
$$

where $Q(e,\hat{\theta}) : \mathbb{R}^{2n_y} \times \mathbb{R}^{n_\theta} \to \mathbb{R}_+$. This leads to

$$
l_\epsilon \geq 2c_1 Q + c_1 \ell_{\gamma_\epsilon}\left(2\|(K^TKG)^T\epsilon\|\right) + c_1(c_1-2)\epsilon^T K^T K R_\epsilon^{-1} K^T K \epsilon \quad \text{(A2)}
$$

As $c_1 > 2$, it can be proved that $l_\epsilon > 0$. Thus, J_ϵ is a meaningful cost function that penalises x, ψ_ϵ, and w. Therefore, rearranging Equation (63) yields the derivation of Equation (A3), which is acquired based on the error equivalence in Equation (45), the disturbance alternative in Equation (50), the feedback controller in Equation (59), the adaptive update law in Equation (61), and the definition of ψ_ϵ in Equation (65). The final form of J_ϵ is written as

$$
\begin{aligned}
J_\epsilon(\psi_\epsilon) = \sup_{w\in\mathbb{W}_\epsilon} \Bigg\{ \lim_{t\to\infty} \Bigg[& c_1\tilde{\theta}^T\Gamma\tilde{\theta} + 2c_1\int_0^t \left(\epsilon^T K^T K(F + L_1(x,\psi_\epsilon))\tilde{\theta}\right) \mathrm{d}\tau \\
& + 2c_1 V_{2,0}(e) - 2c_1\int_0^t \Big(\mathrm{L}_f V_{2,0} + \epsilon^T K^T K \\
& \times \left((F + L_1(x,\psi_\epsilon))(\theta - \hat{\theta}) + \psi_\epsilon + Gw\right)\Big) \mathrm{d}\tau \\
& + \int_0^t \left(c_1^2 \epsilon^T K^T K R_\epsilon^{-1} K^T K \epsilon + 2c_1 \epsilon^T K^T K \psi_\epsilon + \psi_\epsilon^T R_\epsilon \psi_\epsilon\right) \mathrm{d}\tau \\
& - \int_0^t \left(c_1\|w\|^2 - 2c_1\epsilon^T K^T K G w + c_1 \ell_{\gamma_\epsilon}\left(2\|(K^TKG)^T\epsilon\|\right)\right) \mathrm{d}\tau \Bigg] \Bigg\} \\
= \sup_{w\in\mathbb{W}_\epsilon} \Bigg\{ \lim_{t\to\infty} \Bigg[& c_1\tilde{\theta}^T\Gamma\tilde{\theta} - 2c_1\int_0^t \left(\dot{\tilde{\theta}}^T\Gamma\tilde{\theta}\right) \mathrm{d}\tau + 2c_1 V_{2,0}(e) \\
& - 2c_1\int_0^t \left(\mathrm{L}_f V_{2,0} + \epsilon^T K^T K\big((F + L_1(x,\psi_\epsilon))\theta + \psi_2 + Gw\right)\Big) \mathrm{d}\tau \\
& - c_1\int_0^t \left(\|w - (K^TKG)^T\epsilon\|^2\right) \mathrm{d}\tau \\
& + \int_0^t \left(\left(\psi_\epsilon + c_1 R_\epsilon^{-1} K^T K\epsilon\right)^T R_\epsilon \left(\psi_\epsilon + c_1 R_\epsilon^{-1} K^T K\epsilon\right)\right) \mathrm{d}\tau \Bigg] \Bigg\}
\end{aligned} \quad \text{(A3)}
$$

$$
\begin{aligned}
J_\epsilon = {} & c_1\tilde{\theta}^T(0)\Gamma\tilde{\theta}(0) + 2c_1 V_{2,0}\big(x(0), e(0), \hat{\theta}(0)\big) \\
& + \int_0^\infty \left(\left(\psi_\epsilon + c_1 R_\epsilon^{-1} K^T K\epsilon\right)^T R_\epsilon \left(\psi_\epsilon + c_1 R_\epsilon^{-1} K^T K\epsilon\right)\right) \mathrm{d}\tau \\
& + c_1 \sup_{w\in\mathbb{W}_\epsilon} \left\{ -\int_0^\infty \left(\|w - (K^TKG)^T\epsilon\|^2\right) \mathrm{d}\tau \right\}
\end{aligned} \quad \text{(A4)}
$$

It can be proved that

$$
\Upsilon_\epsilon = \sup_{w\in\mathbb{W}_\epsilon} \left\{ -\int_0^\infty \left(\|w - (K^TKG)^T\epsilon\|^2\right) \mathrm{d}\tau \right\} \leq 0 \quad \text{(A5)}
$$

and $\Upsilon_\epsilon = 0$ is achieved if and only if the worst-case disturbance $w^\star = (K^TKG)^T\epsilon$ occurs. Therefore, the solution for a minimal J_ϵ is $\psi_\epsilon = -c_1 R_\epsilon^{-1} K^T K\epsilon$, which proves Theorem 3.1.